199

SATELLITE & MESOMETEOROLOGY
RESEARCH PROJECT

Department of the Geophysical Sciences
The University of Chicago

MICROBURST WIND SHEAR

at New Orleans International Airport, Kenner, Louisiana on July 9, 1982

by

T. Theodore Fujita

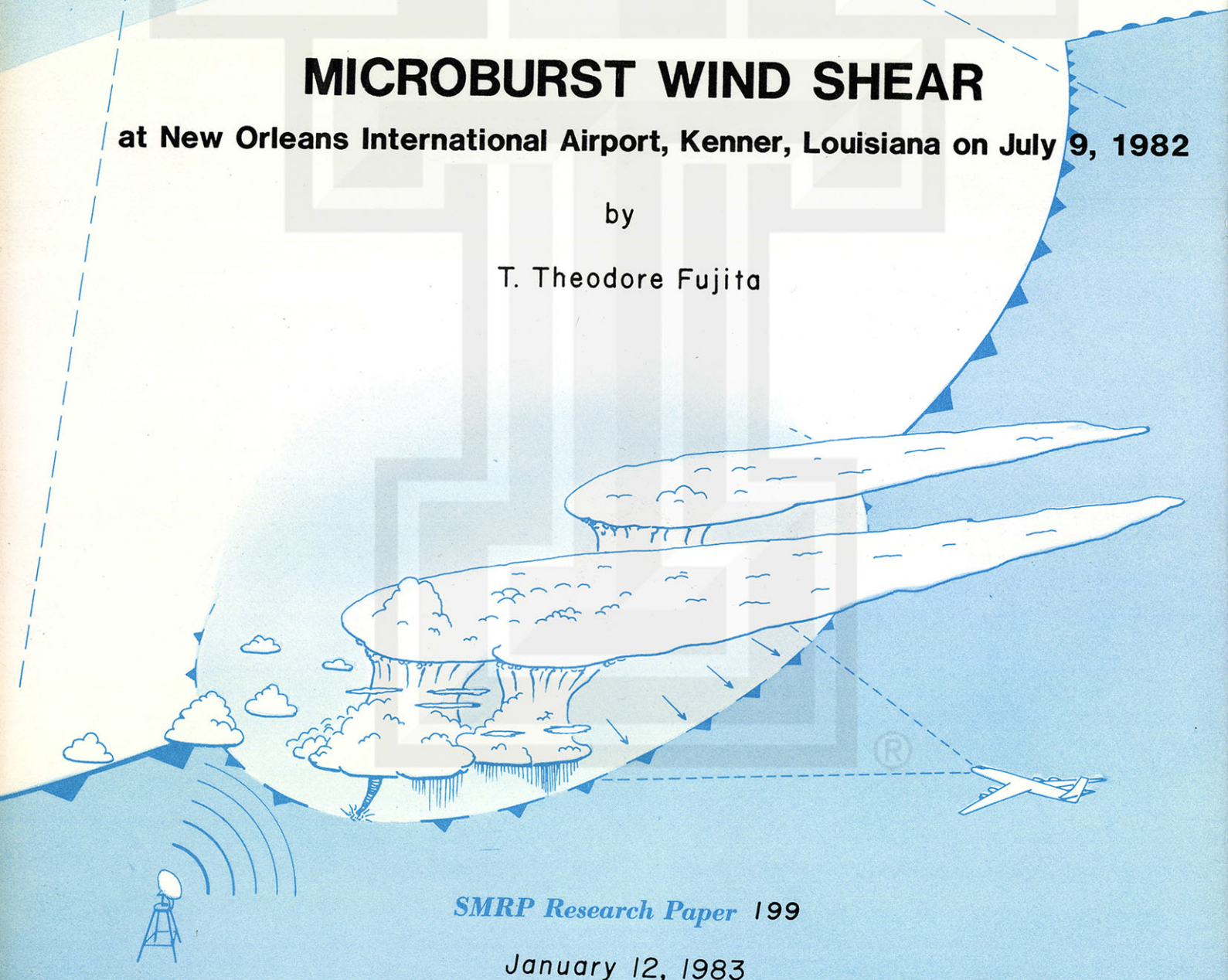

SMRP Research Paper 199

January 12, 1983

MICROBURST WIND SHEAR

at New Orleans International Airport, Kenner, Louisiana, on July 9, 1982.

THE NEW YORK TIMES, MONDAY, JANUARY 17, 1983

Study of Jet Crash Near New Orleans Finds Tree Was a Factor

By RICHARD WITKIN

A jet that crashed last July might have flown safely out of a severe downdraft if there had been no trees in the way, according to a special study prepared for Pan American World Airways.

The Pan Am plane took off from New Orleans' Moisant Airport and had climbed to 163 feet when the strong downdraft caused it to lose altitude rapidly. The pilots of the Boeing 727 had managed to stop the descent and the plane had started climbing again when it struck a tree 52 feet above the ground, the report said.

If the downdraft, called a wind shear or microburst, had been 25 percent weaker, indications are that the aircraft would have missed the trees, according to the study by T. Theodore Fujita, a professor of meteorology at the University of Chicago.

Instead the plane slammed through an area of ranch homes in Kenner, La., less than a mile from the runway. All 146 people on board and eight on the ground were killed.

Expert in Wind Shifts

Mr. Fujita is widely credited with developing the concept of how violent downdrafts can threaten an aircraft at very low altitude. His first major study concerned the crash of a Boeing 727 at Kennedy International Airport in June 1975, in which 113 died.

Mr. Fujita says wind gusting vertically can suddenly shift direction. In such a circumstance the pilot of a plane flying into a headwind would be buffeted by a sharp downdraft and then would quickly have to contend with a tailwind. The sudden slowing of the airflow over the wings, coupled with the downdraft, would mean a loss of lift that could be fatal.

A copy of the Fujita report was obtained by The New York Times from sources close to Pan Am, who said the study would be sent to the National Transportation Safety Board, which is in charge of the inquiry into the crash.

In a telephone interview Friday from his Chicago office, Mr. Fujita said he was optimistic about the chances of developing greatly improved systems for tracking severe wind shifts and warning pilots in time to avoid the area.

"At the least it would be fine if we could save one aircraft," he said.

Wind Bursts on Small Scale

Aviation experts say they are surprised by the small scale of microbursts. Peak winds, according to Mr. Fujita and other researchers, last only one to five minutes and the affected area can be, as it was in New Orleans, only two nautical miles wide. Another surprise has been the discovery that a wind shift can occur in otherwise benign weather.

However, it was raining heavily in the New Orleans area at the time of the crash. Also, several alerts for wind shear conditions, as detected by airport wind monitors, had been broadcast to aircraft, though this was not unusual for the area in July.

By coincidence, Mr. Fujita's University of Chicago research team and a team from the National Center for Atmospheric Research of Boulder, Colo., were in Denver conducting the most ambitious field study to date of the wind-shifting phenomenon when the New Orleans crash occurred.

Officials of the Federal Aviation Administration say the data obtained in the Colorado study will help in the design of new detection and warning systems planned for airports late in this decade.

Displays in Control Tower

A detection system is already in place at more than 60 American airports and the number is to be almost doubled soon. A typical system consists of five or six wind gauges at ground level, with one at the center of the airport and the others a mile or so off the runways.

Displays in the control tower show the wind speed and direction readings of each anemometer. Audio and visual warning devices are set off if the differences among the measurements exceed a certain criterion.

But the system has many shortcomings, chief among them being it only monitors wind close to ground level and only in the areas where the anemometers are situated.

Major hope for an improved warning system lies in the Doppler radar, which can detect wind patterns at considerable distances and altitudes. Much of the data collected in the Colorado study were made possible by Doppler radars.

The new detection system planned for later this decade is a joint effort by the F.A.A., the Commerce Department, and the Department of Defense. Neal Blake, an aviation agency official, said 160 of the new radar systems would be installed.

SMRP Research Paper 199

Satellite & Mesometeorology Reseach Project
Department of the Geophysical Sciences
The University of Chicago

MICROBURST WIND SHEAR

at New Orleans International Airport, Kenner, Louisiana, on July 9,1982

by

Tetsuya Theodore Fujita[1]
Professor of Meteorology
The University of Chicago
Chicago, Illinois 60637

January 12, 1983

---

1. For personal and research references, see "About the author" at the end of this report.

PREFACE

Initially, the author's concept of the downburst (a strong downdraft which induces an outburst of damaging winds on or near the ground), which was originated after the analysis of the JFK accident on June 24, 1975, was regarded as controversial. It was because only a handful of meteorologists, at that time, could visualize that a downdraft descends to as low as 300 ft (100 m) above the ground before spreading out violently. On the contrary, the downdraft, as revealed by the Thunderstorm Project (1946-47), was assumed to lose its downflow speed long before it reaches the ground. Therefore, an aircraft flying beneath a downdraft should not be affected by either downflow or strong outflow winds as long as its flight altitude remains close to the ground.

The gust front, on the other hand, has long been regarded as the inducer of the wind which endangers aircraft during its lift-off and landing operations. In the context of the generalized planetary scale by the author, a gust front is a MESOSCALE (2 to 216 n.m. or 4 to 400 km) front of the cold air which rushes out from beneath thunderstorms.

Fujita and Srivastava of the University of Chicago, as co-investigators, operated the NIMROD (Northern Illinois Meteorological Research On Downburst) Project in 1978 by using three Doppler radars (one located at the O'Hare Airport) and 27 automated surface stations. Approximately 50 downbursts were recorded during the 45 days of the project operation. One of the Doppler radars recorded a peak outflow speed of 62 kts located only 100 to 150 feet above the ground.

JAWS (Joint Airport Weather Studies) Project in 1982 was operated jointly by the University of Chicago and the National Center for Atmospheric Research with Fujita (U of C) and McCarthy and Wilson (NCAR) as co-investigators. One of the Doppler radars was located at Denver's Stapleton Airport. The purpose of this project was to determine the scale, life, and structure of downbursts. Of the numerous downburst winds recorded, 190 were less than 2 n.m. in size, being classified as MISOSCALE (130 to 13,120 ft or 40 to 4,000 m) disturbances.

Based on NIMROD and JAWS researches, the author now sub-classifies the downburst into macroburst and microburst. Their definitions are:

MACROBURST:- A large (mesoscale) sized downburst. An intense macroburst often causes a wide-spread, tornado-like property damage. Damaging winds, lasting 5 to 20 minutes, could reach as high as 150 kts.

MICROBURST:- A small (misoscale) sized downburst with peak winds lasting only 1 to 5 minutes. A microburst induces dangerous tailwind and downflow shear which cannot always be detected by ground-based anemometers.

The purpose of this paper is to clarify the nature of the wind shear which existed at New Orleans International Airport (Moisant Field) at the time of the aircraft accident on July 9, 1982.

T. Theodore Fujita

TABLE OF CONTENTS

Weather Situations at Moisant Airport

Scattered showers were in progress over the New Orleans area on the afternoon of July 9, 1982. The National Weather Service Slidell, LA radar showed the formation, advancement, and dissipation of seven gust fronts (see Fig. 1).

Gust front No. 1, the easternmost one, was tracked only about 10 minutes. No. 2, however, expanded out for almost one hour toward the northwest at the rate of 11 kts. Gust fronts No. 3 and No. 4, identified for about 30 minutes each, also expanded toward the northwest at 10 to 13 kts.

A major gust front No. 5 advanced north-northeast at 19 kts, much faster than the earlier ones. Although the identity of the front was lost in the ground clutter in the New Orleans area, an extrapolated movement indicates that it arrived just to the south of the airport at 2102 GMT when Republic 632 took off toward the south.

The accident aircraft took off at 2108 GMT from runway 10 against a 15 kt headwind from 080°. At that time, gust front No. 6 was approaching the airport area at the rate of 25 kt, which was very fast. The last gust front, No. 7, was also a very fast-moving one.

Satellite pictures reveal the convective activities over the New Orleans area more explicitly than radar pictures, which include city-induced ground clutter. July 9 was the research rapid-scan day of GOES West geosynchronous satellite. Both visible and infrared pictures on digital printouts were being processed to determine variations of clouds at 3-minute intervals.

Four satellite pictures shown in Figs. 2 through 5 are visible images from GOES East. Cold cloud tops are depicted by the infrared gray scale which gradually changes from black to white within two different temperature ranges, -43°C to -60°C and -60°C to -80°C. White changes into black at -43°C and also at -60°C.

Small convective clouds began forming along the lake-breeze front of Lake Pontchartrain which is cloud-free due to relatively cool water temperature. Numbers 1 through 7 in the satellite pictures identify the parent thunderstorms which induced the gust fronts No. 1 through 7 in Fig. 1. Note that storms 1, 2, 3, and 4 dissipated, being taken over by storms 5 and 6, which induced the gust fronts that advanced toward Moisant Field.

It was at 2110 GMT, very close to the accident time, when the cloud top colder than -43°C was first depicted by infrared temperature over the airport area. Until then, the cloud-top temperature was relatively warm indicating that thunderstorm activities had been minor.

In an attempt to show mesoscale (not misoscale) variations of weather parameters at Moisant Airport, pressure, winds and precipitation traces from the National Weather Service at the terminal building were enlarged and put together into Fig. 6. The middle diagram shows the gust recorder trace from the NWS anemometer located near the centerfield LLWSAS anemometer. The sea-level pressure at the top reveals that there were pre- and post-gustfrontal pressure domes.

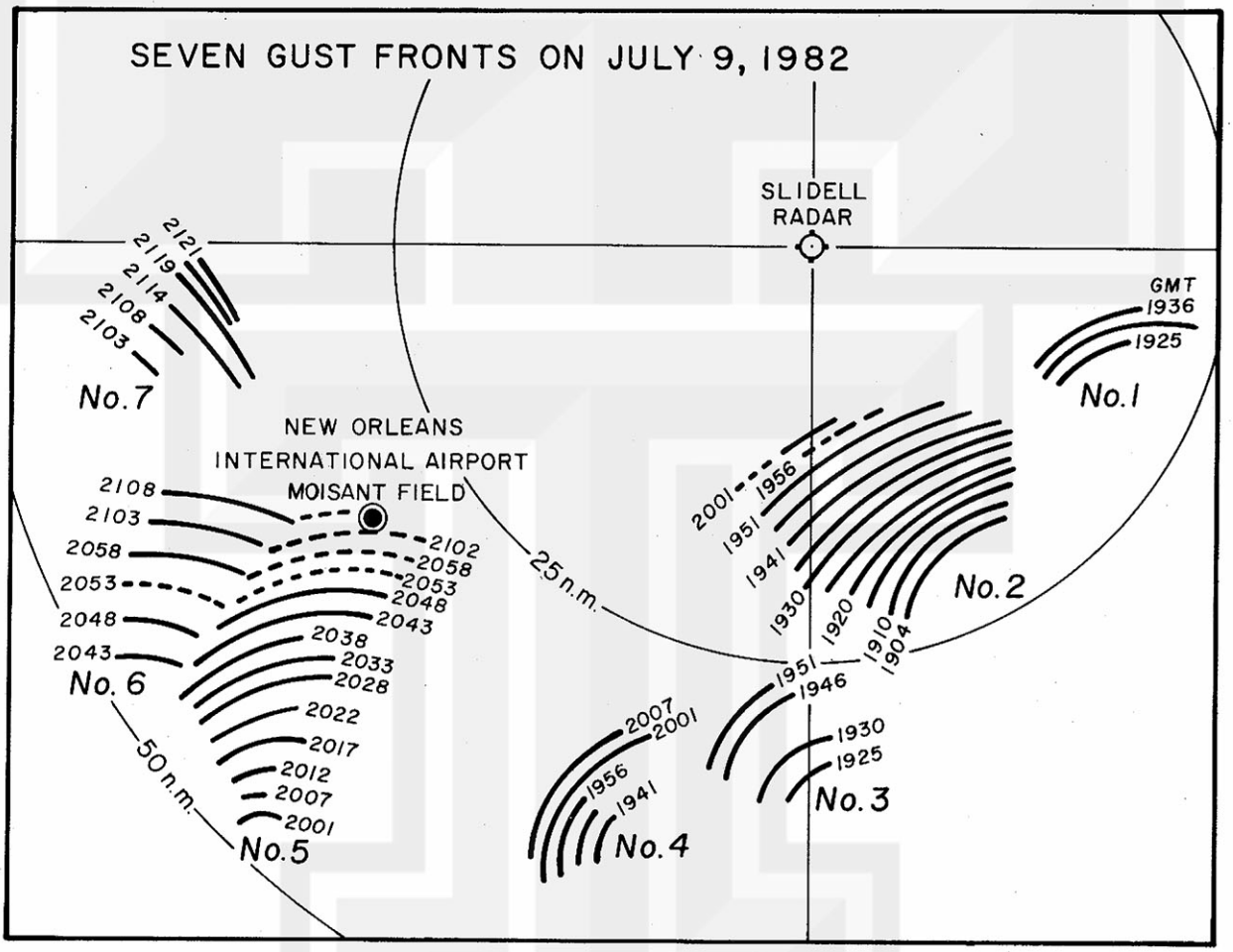

Fig.1 Seven gust fronts on July 9, 1982 determined as based on the radar film from the National Weather Service Office, Slidell, LA. Location and movement were obtained by time-motion analyzer at the University of Chicago.

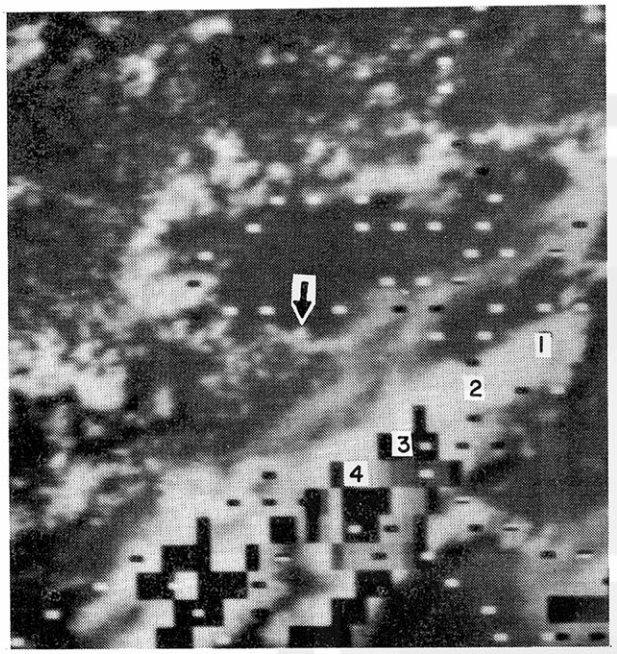

Fig.2 GOES East photograph at 1940 GMT on July 9, 1982. The east-west dimension of the picture coverage is approximately 75 n.m.. Lake Pontchartrain appears dark gray because of suppressed convection by cool water temperature.

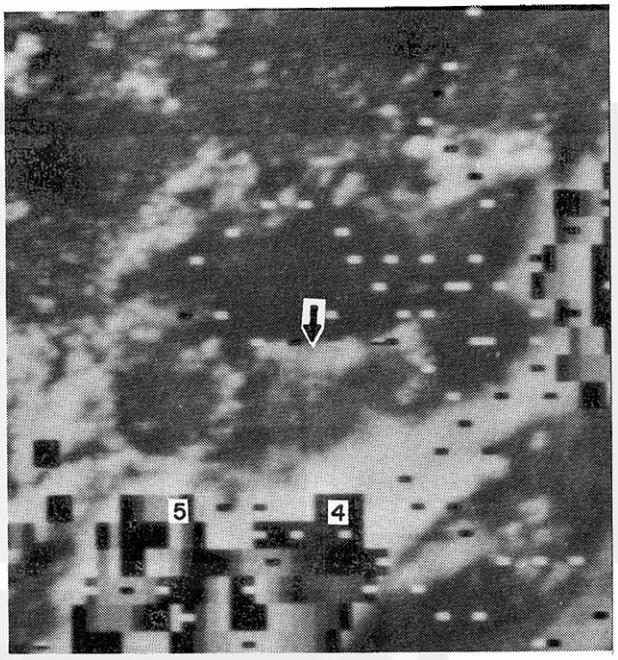

Fig.3 Satellite photograph at 2010 GMT. Numbers in the picture indicate the parent thunderstorms which induce the gust fronts with identical numbers. An arrow in the picture points toward Moisant Airport.

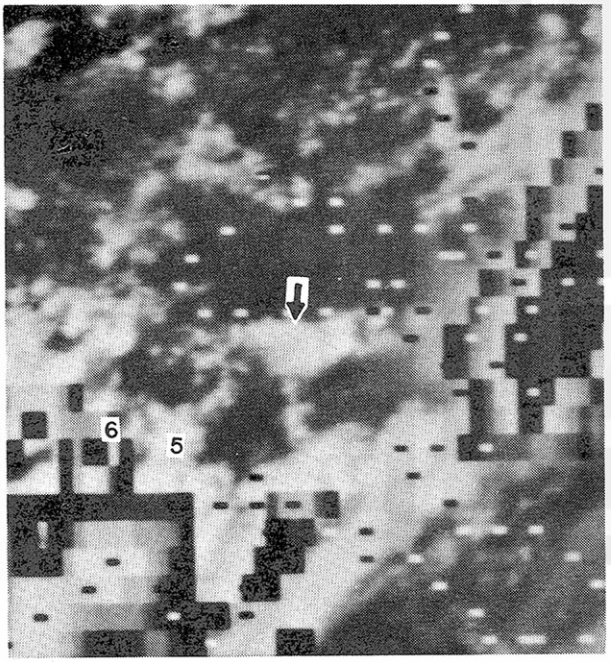

Fig.4 Satellite photograph at 2040 GMT. Storms 5 and 6 induced gust fronts Nos. 5 and 6 which moved toward the airport.

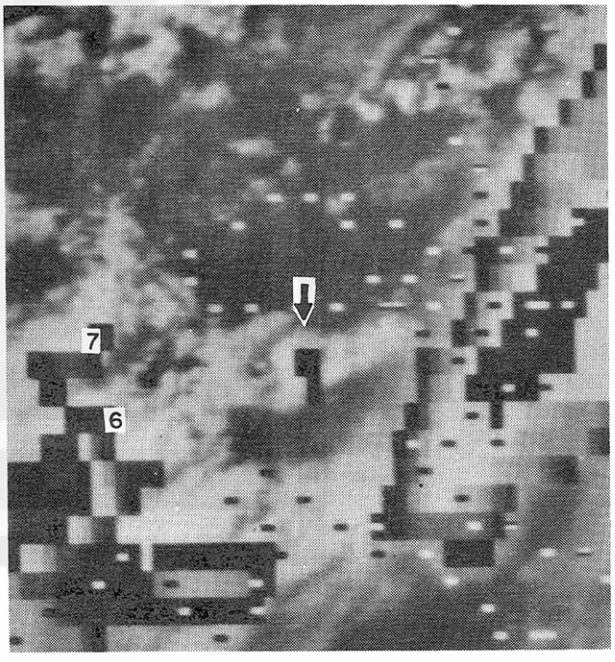

Fig.5 Satellite photograph at 2110 GMT when the accident occurred. Note the formation of the -43°C cloud.

It rained heavily, with the rate up to 5 inches per hour, inside the post-gust-frontal dome.

Two aircraft took off from runway 19 a few minutes before the accident at 2109 GMT. Republic 632 (see Fig. 6) reported strong crosswind from the east and some tailwind while accelerating on the runway. It rotated at 121 kts (11 kts below V1 air speed) and flew into gust front No. 5. Indicated airspeed increased to 160 kts almost instantly. The gust front saved the aircraft by adding to the air speed.

Texas International 794 took off from runway 19 three minutes after Republic 632. It encountered light to moderate rain on the runway but there was no wind shear. While flying across the Mississippi River, the captain commented high wind conditions on "riverboat". The river is located less than a mile from the departure end of runway 19. Fig. 6 suggests the existence of a strong southerly wind just to the south of the airport. The gust-recorder trace shows that the TXI 794 took off during a brief (one minute or so) lull period of gusty wind.

JAWS microbursts reach their mature stage within only 2 to 3 minutes. They simply descend to the ground without showing a detectable wind on the ground even one minute before the initial contact stage. If we generalize this abrupt onset of the microburst winds on the surface, a 4-minute period between 2104 GMT (TXI departure) and 2108 GMT (PAA departure) was long enough for the formation of a microburst in the runway area of Moisant Airport.

An analysis of weather situations presented in this section suggests strongly that the scale of the wind shear which affected the PAA 759 flight cannot be depicted by the so-called mesoanalysis dealing mainly with mesoscale disturbances.

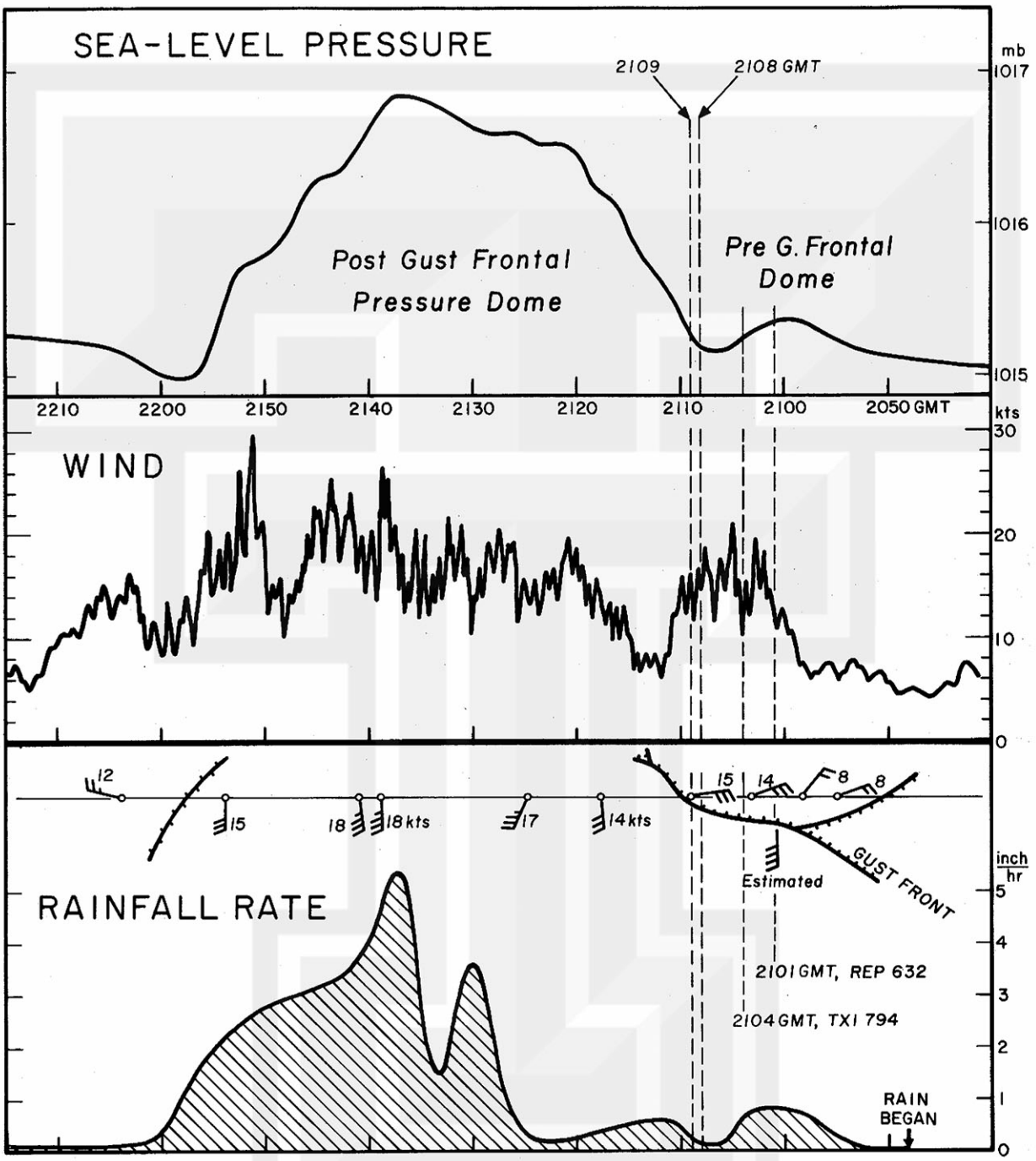

Fig.6 Enlarged traces of pressure, wind, and rainfall rate at Moisant Airport between 2040 and 2215 GMT on July 9, 1982. The airport was under the influence of ENE to NE winds during the pre-gust frontal dome period. After the passage of gust fronts Nos.5 and 7, up to 30 kts gusts from the southerly direction dominated the airport area. Republic 632 was saved by the gust front while Texas International 794 reported no wind shear. PAA 759 released brakes at 2107:56 and made the first contact with trees at 2109:00.

2 Basic Equations for Aircraft Performance Analysis

Analysis of the weather situation at Moisant Field in Section 1 indicated that PAA 759 was affected by a wind disturbance which was too small to be depicted by either satellite or radar photographs which were produced operationally. In other words, the scale of the airflow in question was misoscale (read as myso-scale) which is two orders of magnitude smaller than mesoscale disturbances.

In order to perform a misoscale analysis of the wind system, a complete examination of the aircraft performance is required. For this purpose, a set of basic equations of motion was obtained by using the terms defined in Fig. 7. Four acceleration terms are:

(i) Gravitational Acceleration

The gravitational acceleration g pointing toward the nadir is given by

$$g = 9.80616(1 - 0.00264 \cos 2\phi) \quad m/sec^2 \tag{1}$$

where ϕ is the latitude. Using $\phi = 30.0°$, the gravitational acceleration at Moisant Field is given by

$$9.79\ m/sec^2 = 32.1\ ft/sec^2. \tag{2}$$

(ii) Thrust Force Acceleration

Thrust forces of one CENTER and two POD engines were added in determining three constants, C_1 , C_2 , and C_3 in

$$a_T = k(C_1 + C_2\, e^{-C_3 T}) \tag{3}$$

where T denotes true air speed and k, the factor which varies with minimum, average, and above-average engine thrust. The value of k used in this analysis was obtained from "A performance analysis of Pan American Flight 759 based on NTSB FDR readout dated 10/06/82".

(iii) Lift Force Acceleration

The lift force acceleration applicable to the 727-200 aircraft was expressed by an analytic equation with constants C_4, C_5, C_6, C_7, and C_8.

$$a_L = (1 + C_4 Z^{-1})(C_5 + C_6\alpha - C_7\alpha^{C_8})\, T^2 \tag{4}$$

where Z is the altitude of the aircraft, and α, the angle of attack measured from the fuselage direction. The angle of attack of the wings is 2° larger. A multiplier constant, C_4, determines the effect of the ground upon the lift force acceleration. When the center of gravity of the aircraft is assmued to be 9 ft, C_4 increases from 0.274 to 0.548 corresponding to the 10% to 20% increase in the lift force, respectively. By assuming a 20% increase, $C_4 = 0.548$ is used

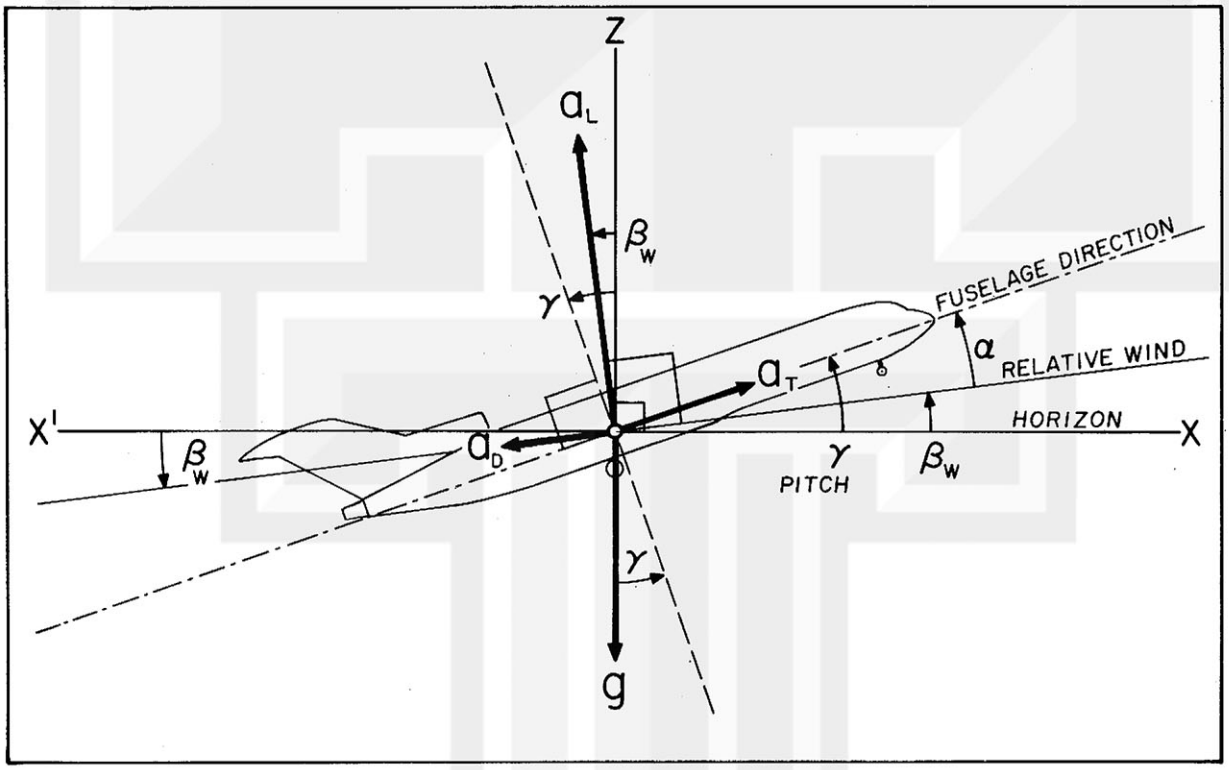

Fig.7 Four accelerations on a flying aircraft. Aircraft's pitch attitude is expressed by γ, angle of attack by α, and the elevation angle of the impinging wind by β_w.

in this paper.

(iv) Drag Force Acceleration

The drag force acceleration is expressed by three different values. They are

$$a_{D1} = (C_9 + C_{10}\alpha^{C_{11}})\, T^2 - C_{12} a_Z \qquad \text{on runway} \tag{5}$$

$$a_{D2} = (C_9 + C_{10}\alpha^{C_{11}})\, T^2 \qquad \text{in the air, gear down} \tag{6}$$

$$a_{D3} = (C_{13} + C_{10}\alpha^{C_{11}})\, T^2 \qquad \text{in the air, gear up} \tag{7}$$

where C_9, C_{10}, C_{11}, C_{12}, and C_{13} are constants and a_Z is the vertical acceleration of the aircraft computed from

$$a_Z = a_T \sin\gamma - a_D \sin\beta_W + a_L \cos\beta_W - g. \tag{8}$$

β_W, identified as β_{wind}, is expressed by

$$\beta_W = \gamma - \alpha \tag{9}$$

where γ is the pitch attitude of the fuselage (see Fig. 7 for definitions).

The FDR acceleration a_F is the acceleration in the direction perpendicular to the fuselage direction. It can be expressed by

$$a_F = a_L \cos\alpha + a_D \sin\alpha - g\cos\gamma \tag{10}$$

which is different from the true vertical acceleration of the aircraft given by Eq. (8). This means that a time integration,

$$\int_o^t a_F \, dt \tag{11}$$

does not represent the aircraft altitude. Instead, we have to write

$$Z = Z_o + \int_o^t a_Z \, dt \tag{12}$$

to compute the altitude Z, noting that the negative value of a_Z computed from Eq. (8) should be changed into "zero" because the negative acceleration is supported by the landing gear.

Various parameters of winds and aircraft motions shown in Fig. 8 are defined as:

u -- headwind, (+)headwind and (-)tailwind

v -- crosswind, (+)toward the left and (-)toward the right

w -- vertical wind, (+)upward and (-)downward

G -- ground speed measured on the horizontal plane

G_X -- ground speed measured in the runway direction

G_Y -- ground speed measured perpendicular to the runway direction

G_Z -- Vertical speed of aircraft

A -- aircraft speed measured on the vertical plane

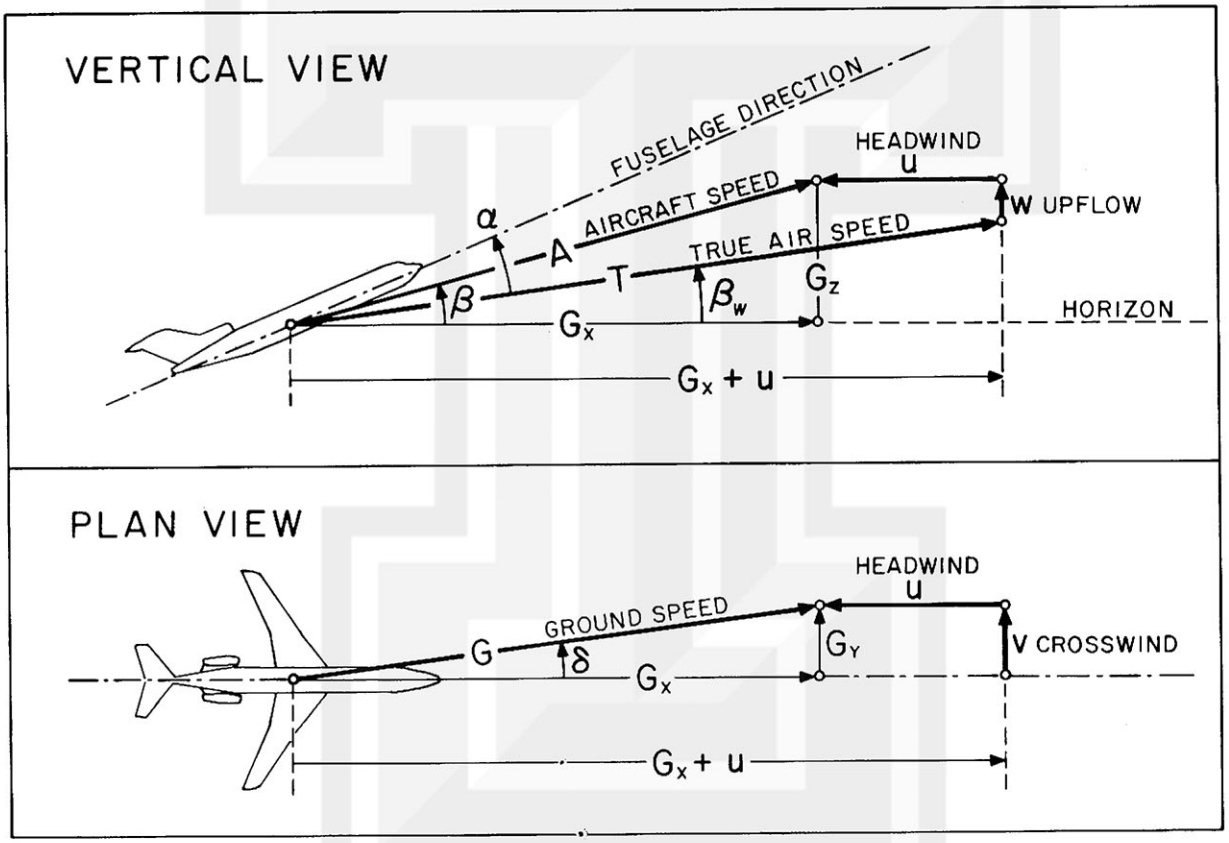

Fig.8 Navigation and wind triangles applicable to an aircraft flying through a wind field expressed by u, v, and w components. The elevation angle of the aircraft velocity β is different from β_w which increases with tailwind and downflow speeds.

3 Eight Constraints for the Performance Analysis

The foregoing equations can be used in computing various aircraft parameters such as speed and altitude of the aircraft from the brake release to the first impact. Without realistic constraints, however, there will be an unlimited number of solutions corresponding to possible assumptions. For this purpose, eight constraints were used to come up with a unique solution of the flight performance presented in this paper.

CONSTRAINT [1] • The time between the brake release (t = 0) and the first contact (t = 1) should be

$$t = 2109{:}00 - 2107{:}56 = 64 \text{ sec.} \tag{13}$$

Plus or minus one second difference is permissible in view of the possible time error of the FDR readout. Table 1 shows the time of events from EXHIBIT No. 12-A.

CONSTRAINT [2] • Distance from the brake release to the first-contact tree should be

$$X_1 = \int_0^{t_1} G_X \, dt = 11{,}525 \text{ ft.} \tag{14}$$

CONSTRAINT [3] • Cross-runway distance of the first-contact tree should be

$$Y_1 = \int_0^{t_1} G_Y \, dt = 172 \text{ ft.} \tag{15}$$

The FDR readout indicates that the aircraft kept its heading toward the left of the runway heading. There was a considerable difference between the aircraft heading and the ground-track heading, indicating that the aircraft flew through a crosswind blowing from the left side of the runway.

An analysis of the crosswind situation is presented in Fig. 9. The figure shows that the FDR heading of the aircraft, while rolling toward the rotation, was 98.9°; while the magnetic heading of the runway 10 is 102.37°. In plotting the ground-track headings after the first impact, they were adjusted to the FDR heading shown on the right edge of the figure. The ground-track heading from the brake release to the rotation should be connected to the post-impact heading. The connection was achieved by equating two areas A and B to that of A + B in the figure.

The difference between the aircraft heading (FDR heading) and the ground-track heading is resulted by the crosswind v which can be computed from

$$v = G'_X \tan \delta \tag{16}$$

where δ denotes the drift angle and G'_X the ground speed of the aircraft in the direction of the fuselage. G'_X is identical to G_X if there were no crosswind.

Table 1 TIME OF EVENTS from EXHIBIT No. 12-A.
Cockpit voice recorder timing is accurate to one second.

Events	GMT Time sec	X ft	Y ft	Z ft
End of RWY 10	-------	-80	0	0
Brake release	2107:56	0	0	9
Takeoff thrust	2107:59	-	0	9
Windshield wiper on	2108:06	-	0	9
Wiper speed increases	2108:27	-	0	9
Rotation	2108:33	-	0	9
Gear up started	2108:42	-	-	-
V 2 speed	2108:43	-	-	-
You're sinking	2108:45	-	-	-
GPWS	2108:57	-	-	-
First impact	2109:00	11525	172	52
Ground impact	2109:04	12890	411	54
End of tape	2109:05	-	-	-

X is measured from the brake release point (assumed 80 ft from the end of RWY 10) toward the center line of the runway.

Y is the cross-runway distance. Positive toward the left (north-northeast)

Z is the height above the runway surface. Z = 9 ft is the height of the center of gravity of the aircraft while on the runway.

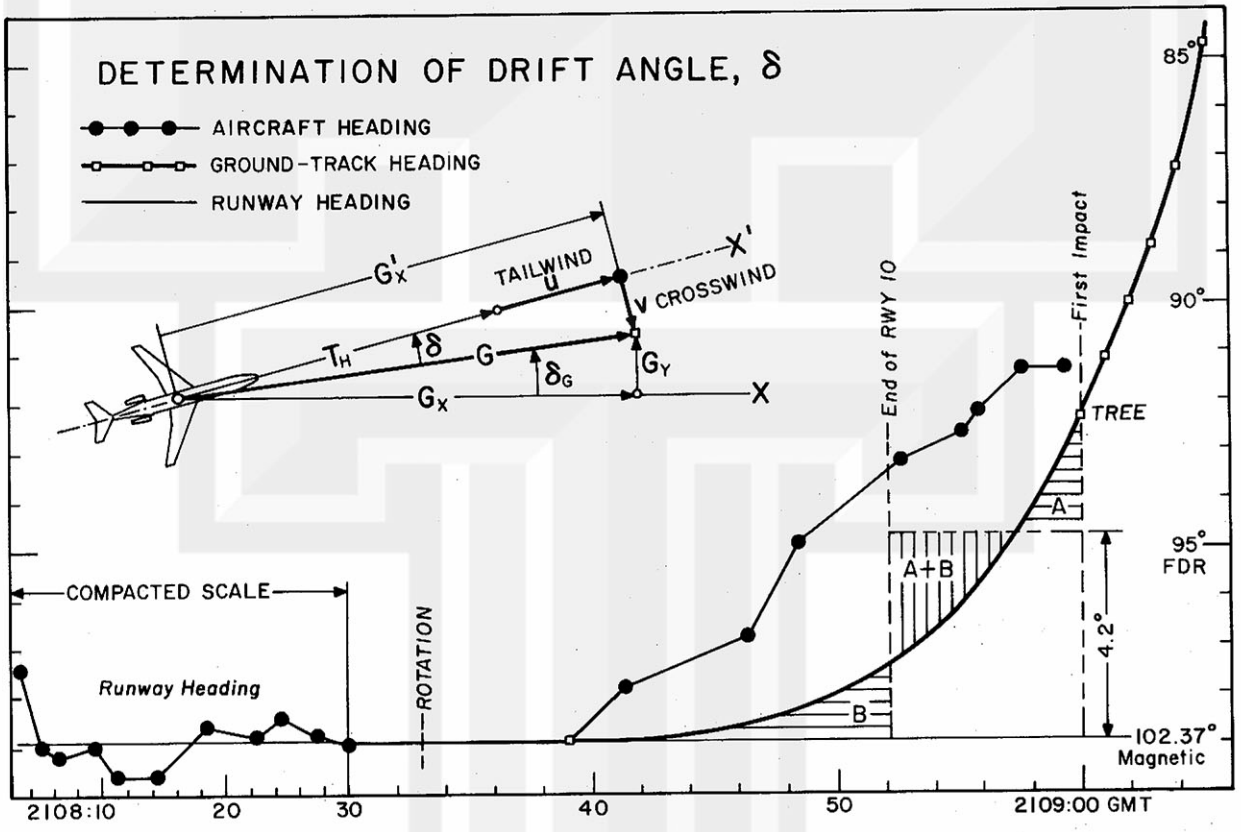

Fig. 9 Determination of crosswind based on the drift angle computed as the difference between the aircraft heading and the ground-track heading. When drift angle is zero, the direction of X' coincides with the runway direction X.

CONSTRAINT [4] • Impact height of the first-contact tree should be

$$Z_1 = Z_o + \int_o^{t_1} G_Z \, dt = 52 \text{ ft} \tag{17}$$

where Z_o = 9 ft and G_Z the vertical speed of the aircraft. This constraint should be met with a possible error of 1 to 2 ft. Otherwise, the aircraft does not impact the huckleberry tree at the measured height.

CONSTRAINT [5] • Evidence of the damage to trees located between Williams and Clay Streets shows that the aircraft was climbing when the first contact occurred. The estimated rate of climb based on Fig. 10 is

$$\left(\frac{dZ}{dt}\right)_{t_1} = 430 \pm 100 \text{ fpm}, \tag{18}$$

indicating that the aircraft could have flown out of the microburst if there were no trees there. This boundary condition of the positive climb rate at $t = t_1$ should be met in order to reconstruct the realistic flight path.

CONSTRAINT [6] • The most important but often neglected constraint is the coupling of vertical and horizontal winds obtained by an aircraft performance analysis. In other words, u, v, and w should be interlinked by the equation of continuity which can be expressed by

$$\frac{dw}{dZ} = -\left(\frac{du}{dX} + \frac{dv}{dY}\right) \tag{19}$$

which will result in a strict constraint,

$$w = -\int_o^Z \text{div (horizontal wind)} \, dZ \tag{20}$$

which means that all disturbances, without exceptions, must be characterized by the interlinked horizontal and vertical winds. It will be seen later that +17 to -31 kts horizontal wind shear requires a vertical wind of 7 fps or approximately 4 kts at about 150 ft above the runway. A 10 kt downflow will induce +42 to -77 kts or 119 kts wind shear which could blow down some trees in the airport area.

CONSTRAINT [7] • Reconstruction of the FDR true air speed should be achieved. Because of the fact that the indicated air speed is computed by the differential pressure between the Pitot tube and the static ports, it is necessary to compute the true air speed T from

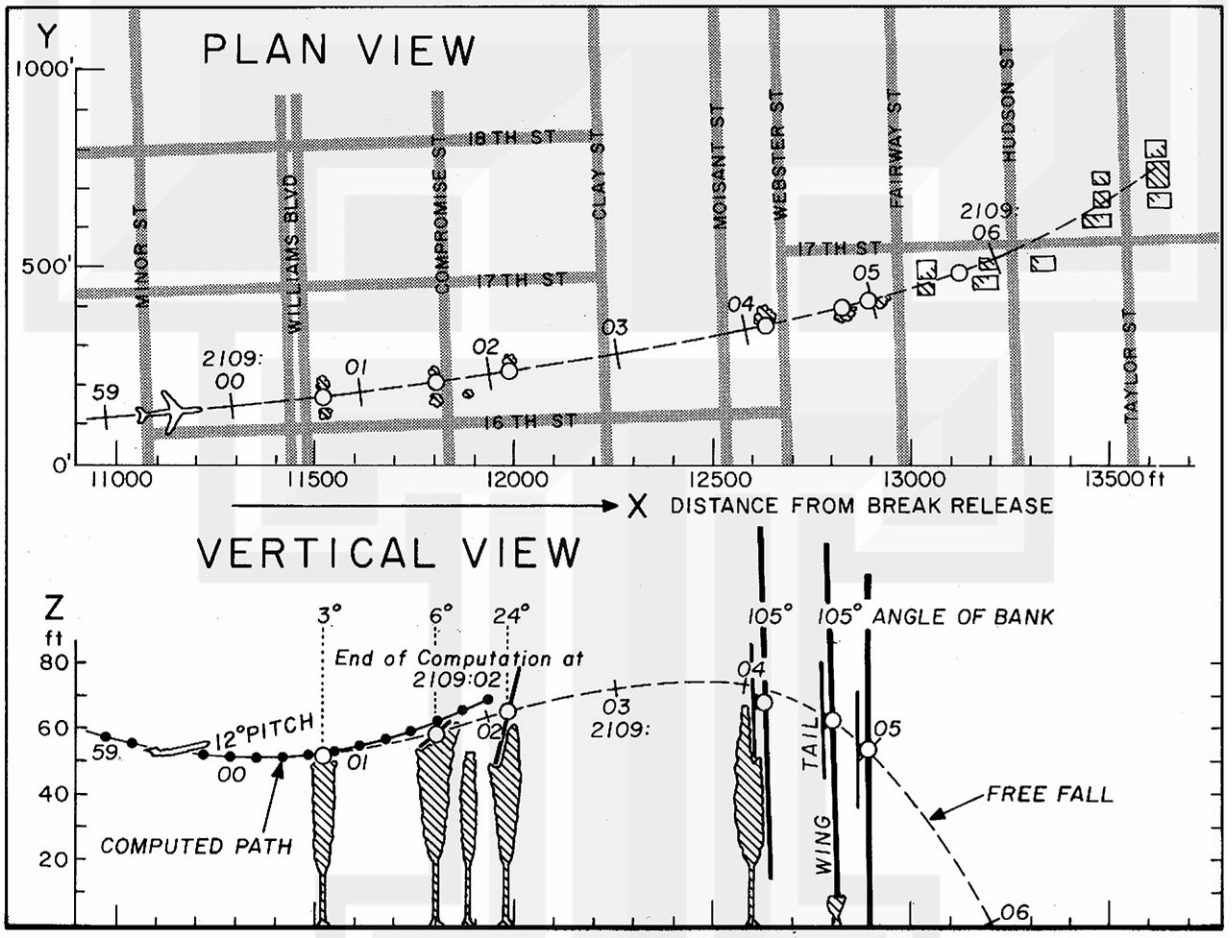

Fig.10 Estimated movement of the center of gravity of the aircraft after its first contact with three trees on the east side of Williams Blvd. The rate of climb of the aircraft was approximately 430 feet per minute at the first contact. At about 2109:03, the flying capability of the aircraft was lost, descending at free-fall rate thereafter.

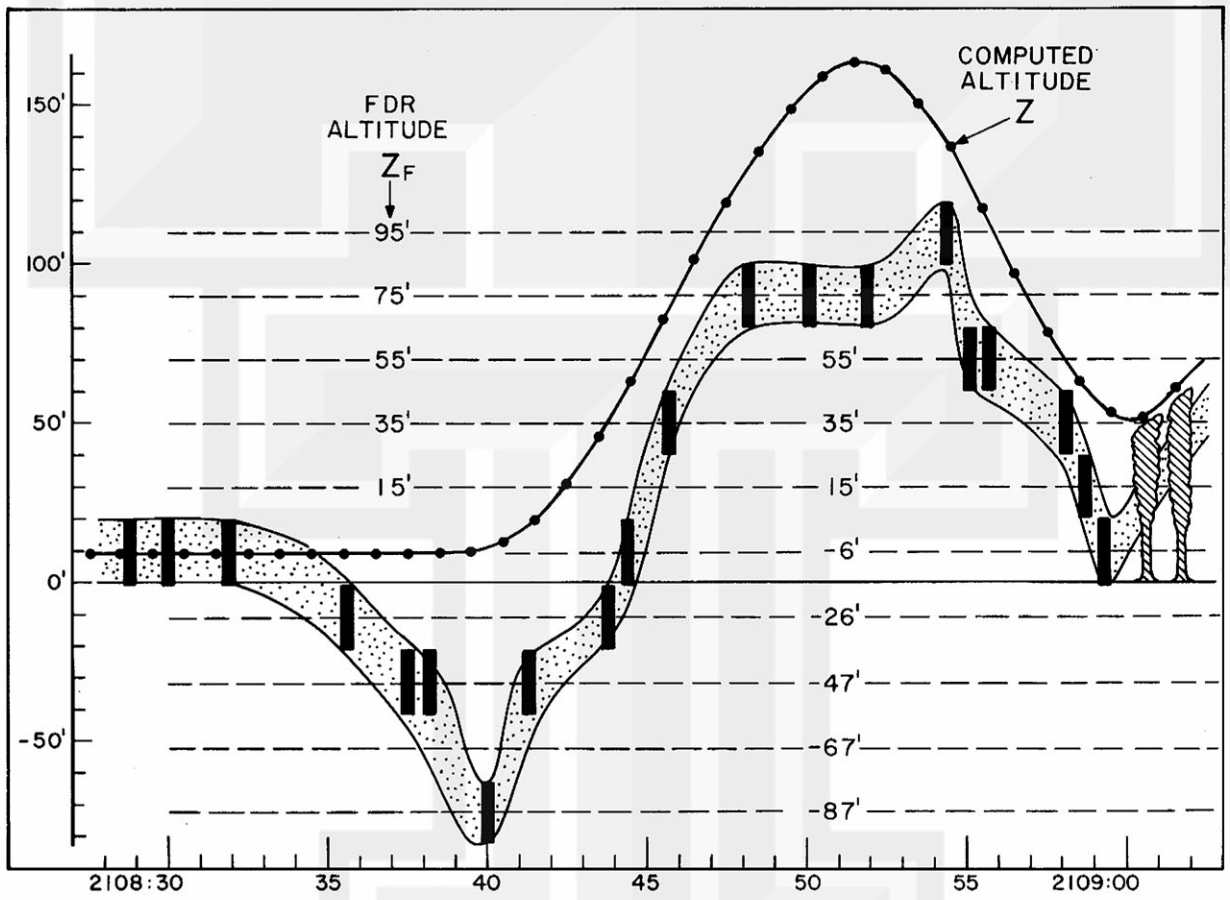

Fig.11 Flight Data Recorder (FDR) altitudes which were shifted up to coincide with 9 ft above the runway. The FDR altitude dip is resulted by the static ports pressure which increases when the pitch attitude increases prior to the liftoff. As the aircraft altitude increases, the static ports pressure approaches the true static pressure. The FDR altitude dip near the peak altitude of 163 ft connot be explained aerodynamically. It could, however, be the misoscale high pressure caused by the downflow as it slows down while approaching the ground.

$$T^2 = \frac{\rho_o}{\rho} I^2 + 2\, g\, \Delta Z \qquad (21)$$

where $\rho_o = 1.2255$ kg/m^3 is the density of the standard atmosphere at sea level, ρ, the density at the airport, and ΔZ the pressure height decrease corresponding to the increase in the static port pressure. Under normal conditions, ΔZ increases rapidly from the rotation to the liftoff location where it reaches the peak value of 50 to 100 ft. Thereafter, it decreases rapidly to zero as the aircraft altitude increases.

Fig. 11 was used to obtain ΔZ as a function of time, assuming that ΔZ decreases to zero when the aircraft altitude exceeds 100 ft. In computing the true air speed in Table 2, Eq. (21) was modified into

$$T = (1.05\ I^2 + 22.5\, \Delta Z)^{\frac{1}{2}} \qquad (22)$$

in which ΔZ is in ft, and both T and I are in kts. It should be noted that the maximum difference between T and I was 9 kts at 2108:40, the time of liftoff (see Table 2).

CONSTRAINT [8] • Reconstruction of the FDR acceleration should be achieved. While satisfying the seven constraints listed above, we will still be able to alter the flight track, both horizontally and vertically, with some degree of freedom. This constraint, when applied strictly, will result in a unique solution which will faithfully reconstruct all flight conditions experienced by PAA 759.

ESTIMATED TEMPERATURE AND PRESSURE
IN MICROBURST FOR DENSITY COMPUTATION

Air temperature 81°F (27°C)

Dew-point temperature 73°F (23°C)

Virtual temperature 27°C + 3°C = 30°C = 303°k

Atmospheric pressure 1015.2 mb

Computed density of the air 1.1671 kg/m^3

Table 2 COMPUTATION OF TRUE AIR SPEED

True air speed, T was computed as a function of I, indicated air speed and $\Delta Z = Z - Z_F$, altitude dip due to the increase in the static ports pressure. Density of the air was assumed to be 1.167 kg/m³.

GMT	Time sec	I kts	Z ft	Δ Z ft	T kts	T − I kts
2107:	59.3	13	9	0	13	0
2108:	03.7	31	9	0	32	1
	07.5	41	9	0	42	1
	10.0	50	9	0	51	1
	13.1	66	9	0	68	2
	16.9	78	9	0	80	2
	18.7	91	9	0	93	2
	21.2	100	9	0	102	2
	22.5	105	9	0	108	3
	23.7	113	9	0	106	3
	26.3	118	9	0	121	3
	28.1	124	9	0	127	3
	30.6	128	9	0	131	3
	31.3	133	9	0	136	3
	32.5	135	9	0	138	3
	33.?	Rotation				
	33.8	140	9	0	143	3
	35.6	144	9	10	148	4
	36.9	142	9	20	147	5
	37.5	145	9	30	151	6
	38.2	147	9	40	153	6
	39.4	153	9	60	161	8
	40.0	160	10	80	169	9
	40.7	159	13	60	167	8
	41.3	156	18	50	163	7
	42.5	158	30	50	165	7
	44.5	151	61	50	158	7
	45.0	154	73	30	159	5
	45.7	155	86	20	160	5
	46.3	158	97	10	163	5
	48.8	156	139	0	160	4
	49.4	153	147	0	157	4
	50.1	149	155	0	153	4
	50.7	147	160	0	151	4
	53.8	146	146	0	150	4
	54.4	142	138	0	145	3
	55.1	145	125	0	149	4
	55.7	149	113	0	153	4
	57.5	151	78	10	155	4
	58.7	159	60	20	164	5
	59.3	160	54	30	165	5
2109:	00.?	FIRST IMPACT				

4 Computations with 0.1 Second Time Steps

In computing the flight parameters through step-by-step integration, the parameters for the first 5 seconds were obtained by hand calculations. The chronological events which took place from the moment of brake release were assumed to be

2107:56 Brake was released at this time, 80 ft from the approach end of RWY 10.

2107:59 Takeoff thrust was applied. Thrust was 67.5% of the takeoff thrust for the first 1.1 seconds and 97.5% for the next 1.4 seconds.

2108:01.5 100% thrust acceleration began.

2108:02.0 0.1 second time-step computation starts by using hand-calculated values as input: X = 48', Y = 0', Z = 9', G_X = 14.4 kts.

Input Values at One-Second Intervals

In performing the step-by-step integration, three basic parameters were selected. They are: (a) Pitch attitude γ, (b) Headwind speed u, and (iii) vertical flow speed w. Each of these parameters was kept constant for one second before assigning a new value at the beginning of the next second.

Each second was divided into ten 0.1 second time steps for computing both horizontal and vertical accelerations at time t

$$[a_X = a_T \cos\gamma - a_D \cos\beta_W - a_L \sin\beta_W]_{at\ t} \tag{21}$$

$$[a_Z = a_T \sin\gamma - a_D \sin\beta_W + a_L \cos\beta_W - g]_{at\ t} \tag{22}$$

Both a_X and a_Z were kept constant during the following 0.1 second for computing the increments of both horizontal and vertical velocities.

$$[\Delta G_X = a_X \times 0.1\ \text{sec}]_{t\ to\ t+0.1} \tag{23}$$

$$[\Delta G_Z = a_Z \times 0.1\ \text{sec}]_{t\ to\ t+0.1} \tag{24}$$

which were used to compute the increments of both X and Z, from

$$[\Delta X = G_X \times 0.1\ \text{sec}]_{t\ to\ t+0.1} \tag{25}$$

$$[\Delta Z = G_Z \times 0.1\ \text{sec}]_{t\ to\ t+0.1} \tag{26}$$

The increment values computed from Eqs. (23) through (26) were then used in determining

$$[\ G_X\ ]_{t+0.1} = [\ G_X\ ]_t + [\Delta G_X]_{t\ to\ t+0.1} \tag{27}$$

$$[\ G_Z\ ]_{t+0.1} = [\ G_Z\ ]_t + [\Delta G_Z]_{t\ to\ t+0.1} \tag{28}$$

$$[\ X\ ]_{t+0.1} = [\ X\ ]_t + [\Delta X\ ]_{t\ to\ t+0.1} \tag{29}$$

$$[\ Z\ ]_{t+0.1} = [\ Z\ ]_t + [\Delta Z\ ]_{t\ to\ t+0.1} \tag{30}$$

Both a_X and a_Z in Eqs. (21) and (22) include T, α , and β_W as well as the input values γ , u, and w. These values computed from

$$[\ T\ ]^2_{t+0.1} = [\ G_X + u\ ]^2_{t+0.1} + [\ G_Z - w\ ]^2_{t+0.1} \tag{31}$$

$$[\ \beta_W\ ]_{t+0.1} = \tan^{-1}\left[\frac{G_Z - w}{G_X + u}\right]_{t+0.1} \tag{32}$$

$$[\ \alpha\ ]_{t+0.1} = [\ \gamma\ ]_{t+0.1} - [\ \beta_W\ ]_{t+0.1} \tag{33}$$

are put into Eqs. (21) and (22) to repeat computations for determining parameters at t + 0.2 seconds. A total of 600 computation steps are repeated for obtaining computed values of T, G_X, G_Z, α , X, Z, and other parameters.

As expected, the first guess input failed to satisfy none of the eight constraints listed in Section 3. As the iterated inputs improved, the results began satisfying the number of constraints one by one. Finally, the 27th iteration resulted in a unique solution which reconstructed the flight under investigation (see Table 3 for the input and computed values).

Both input and output values in Table 3 are presented in graphical forms in Figs. 12 and 13. The significant results seen in these figures and table satisfy the following constraints:

CONSTRAINT [1] ● Time between the brake release and the first contact is 64.7 seconds, which is 0.7 seconds longer than 64 seconds in Eq. (13), but within the range of the FDR time error.

CONSTRAINT [2] ● Distance from the brake release to the first contact tree is 11,518 ft which is only 7 ft shorter than 11,525 ft, the distance specified in Eq. (14).

CONSTRAINT [3] ● This constraint is not applicable to this computation, but was met in crosswind computations shown later.

CONSTRAINT [4] ● Impact height of the first contact tree is 52.5 ft which is 0.5 ft higher than 52 ft given in Eq. (17).

CONSTRAINT [5] • The rate of climb at the first impact is 361 fpm which is within the range of the rate specified in Eq. (18).

CONSTRAINT [6] • This constraint is satisfied by computing vertical velocities from divergence. The result is presented in the next section.

CONSTRAINT [7] • Reconstruction of FDR true air speed is very good (see Fig. 13). However, the true air speeds computed from FDR is approximately 1 kt higher than computed values. It turned out that the FDR speeds are 1 to 2 kts too high to satisfy Constraint [2] because an increased headwind does reduce the ground speed, making it impossible to hit the first-contact tree within the time limit of Constraint [1].

CONSTRAINT [8] • Reconstruction of FDR acceleration is also very good (see Fig. 13). Computed values reproduced most of the significant changes of the FDR acceleration.

HIGHLIGHTS of the 27th iterative computation are that the computed values reconstruct the air speed and the vertical acceleration from FDR, while satisfying other constraints listed in this paper. These computed characteristics are:

- Aircraft lifted off at 2108:39.2, approximately 6 seconds after rotation.
- The maximum altitude of 163.2 ft was reached at 2108:51.5 followed by the minimum altitude of 50.7 ft at 2109:00.2.
- The first impact tree was hit with a 12° pitch attitude while climbing at 361 feet per minute.
- The maximum 17 kts headwind and 31 kts tailwind were encountered.
- The maximum downflow speed was 7 feet per second or 4.1 kts.
- The pitch attitude gradually increased at 13° then it decreased to 5° before increasing again to 12°.

Table 3 AIRCRAFT PARAMETERS COMPUTED AS FUNCTIONS OF TIME.

Input values: γ pitch attitude of aircraft in deg, u headwind in kts and w updraft in ft/sec. Each input was kept constant during each second.

Output values: T true air speed in kts, G_X horizontal ground speed, G_Z vertical ground speed, α angle of attack in deg, a_F acceleration vertical to fuselage axis in g unit, X distance from point of brake release, and Z height of aircraft above runway.

GMT	Time	γ	u	w	T	G_X	G_Z	α	a_F	X	Z
	sec	deg	kts	fps	kts	kts	fpm	deg	g	ft	ft
2107:	56.?	Brake release									
	56.0	0	0	0	0	0	0	0	1.00	0	9
	57.0	0	0	0	1	1	0	0	1.00	1	9
	58.0	0	0	0	2	2	0	0	1.00	3	9
	59.?	Takeoff thrust									
	59.0	0	0	0	3	3	0	0	1.00	7	9
2108:	00.0	0	0	0	6	6	0	0	1.00	14	9
	01.0	0	0	0	10	10	0	0	1.00	27	9
	02.0	0	+9	0	23	14	0	0	1.00	48	9
	02.5	0	+9	0	26	17	0	0	1.00	61	9
	03.5	0	+9	0	30	21	0	0	1.00	93	9
	04.5	0	+7	0	32	25	0	0	1.00	132	9
	05.5	0	+6	0	36	30	0	0	1.00	179	9
	06.5	0	+5	0	39	34	0	0	1.00	233	9
	07.5	0	+4	0	41	38	0	0	1.00	294	9
	08.5	0	+2	0	44	42	0	0	1.00	362	9
	09.5	0	+2	0	49	47	0	0	1.00	438	9
	10.5	0	+2	0	53	51	0	0	1.00	520	9
	11.5	0	+3	0	58	55	0	0	1.00	609	9
	12.5	0	+4	0	63	59	0	0	1.00	706	9
	13.5	0	+5	0	68	63	0	0	1.00	809	9
	14.5	0	+4	0	71	67	0	0	1.00	919	9
	15.5	0	+3	0	74	71	0	0	1.00	1035	9
	16.?	Eighty knots									
	16.5	0	+3	0	78	75	0	0	1.00	1158	9
	17.5	0	+4	0	82	79	0	0	1.00	1288	9
	18.5	0	+7	0	89	82	0	0	1.00	1424	9
	19.5	0	+9	0	95	86	0	0	1.00	1567	9
	20.5	0	+9	0	99	90	0	0	1.00	1715	9
	21.5	0	+9	0	102	93	0	0	1.00	1870	9
	22.5	0	+9	0	156	97	0	0	1.00	2030	9
	23.5	0	+12	0	112	100	0	0	1.00	2197	9
	24.5	0	+12	0	116	104	0	0	1.00	2369	9

GMT	Time	γ	u	w	T	G_x	G_z	α	a_F	X	Z
	sec	deg	kts	fps	kts	kts	fpm	deg	g	ft	ft
2108:	25.5	0	+10	0	117	107	0	0	1.00	2547	9
	26.5	0	+10	0	120	110	0	0	1.00	2731	9
	27.5	0	+9	0	122	113	0	0	1.00	2920	9
	28.5	0	+9	0	126	117	0	0	1.00	3114	9
	29.5	0	+8	0	128	120	0	0	1.00	3314	9
	30.5	0	+8	0	131	123	0	0	1.00	3519	9
	31.5	0	+9	0	135	126	0	0	1.00	3730	9
	32.5	0	+9	0	138	129	0	0	1.00	3945	9
	33.?	Rotation, Vee R 138 kts IAS									
	33.5	0.1	+9	0	141	132	0	0.1	1.00	4166	9
	34.5	0.3	+9	0	144	135	0	0.3	1.00	4392	9
	35.5	0.6	+8	0	146	138	0	0.6	1.00	4622	9
	36.5	1.5	+5	0	146	141	0	1.5	1.00	4857	9
	37.5	3.0	+4	0	147	143	0	3.0	1.00	5098	9
	38.5	5.0	+7	0	153	146	0	5.0	1.00	5342	9
	39.5	7.0	+14	0	163	149	75	6.7	1.07	5592	9
	40.5	8.0	+17	0	168	151	291	7.0	1.14	5845	12
	41.?	Positive climb									
	41.5	10.0	+11	0	163	152	547	8.1	1.13	6101	19
	42.?	Gear up									
	42.5	11.0	+11	0	164	153	798	8.3	1.14	6359	31
	43.?	Vee two, 151 kts IAS									
	43.5	12.0	+6	-1	161	154	986	8.3	1.07	6619	46
	44.5	13.0	+3	-1	158	155	1113	8.8	1.06	6880	63
	45.?	Come on back you're sinking Don									
	45.5	12.0	+3	-2	159	156	1147	7.5	0.95	7142	83
	46.5	12.0	+5	-2	162	156	1116	7.7	1.00	7406	101
	47.5	11.0	+2	-3	160	157	1031	6.7	0.88	7670	120
	48.5	11.0	+1	-4	160	158	864	7.1	0.91	7937	135
	49.5	11.0	-3	-5	157	160	716	7.3	0.90	8205	148
	50.5	10.0	-9	-6	152	161	478	6.9	0.80	8476	159
	51.5	7.0	-10	-7	153	163	43	5.3	0.69	8750	163
	52.5	7.0	-16	-6	150	166	-408	7.2	0.79	9028	160
	53.5	7.0	-21	-5	148	169	-686	8.5	0.86	9311	150
	54.5	5.0	-28	-4	144	172	-971	7.9	0.79	9599	136
	55.5	5.0	-28	-3	148	176	-1235	9.0	0.90	9893	118
	56.5	7.0	-29	-2	151	180	-1214	11.1	1.08	10194	96
	57.?	GPWS -- Whoop whoop pull up whoop									
	57.5	7.0	-31	-1	153	183	-1016	10.5	1.10	10500	78
	58.5	7.0	-27	0	160	187	-780	9.8	1.13	10813	63
	59.5	9.0	-26	0	164	190	-392	10.4	1.25	11131	53
2109:	00.?	Sound of impact -- huckleberry tree at X = 11,525' Z = 52'									
	00.5	12.0	-26	+1	166	192	+216	11.5	1.38	11453	51
	00.7	12.0	-26	+1	166	192	+361	11.0	1.34	11518	52
	01.5	12.0	-25	+1	168	193	+830	9.4	1.24	11778	61
	02.0	12.0	-25	+1	168	193	+1044	8.7	1.19	11941	69

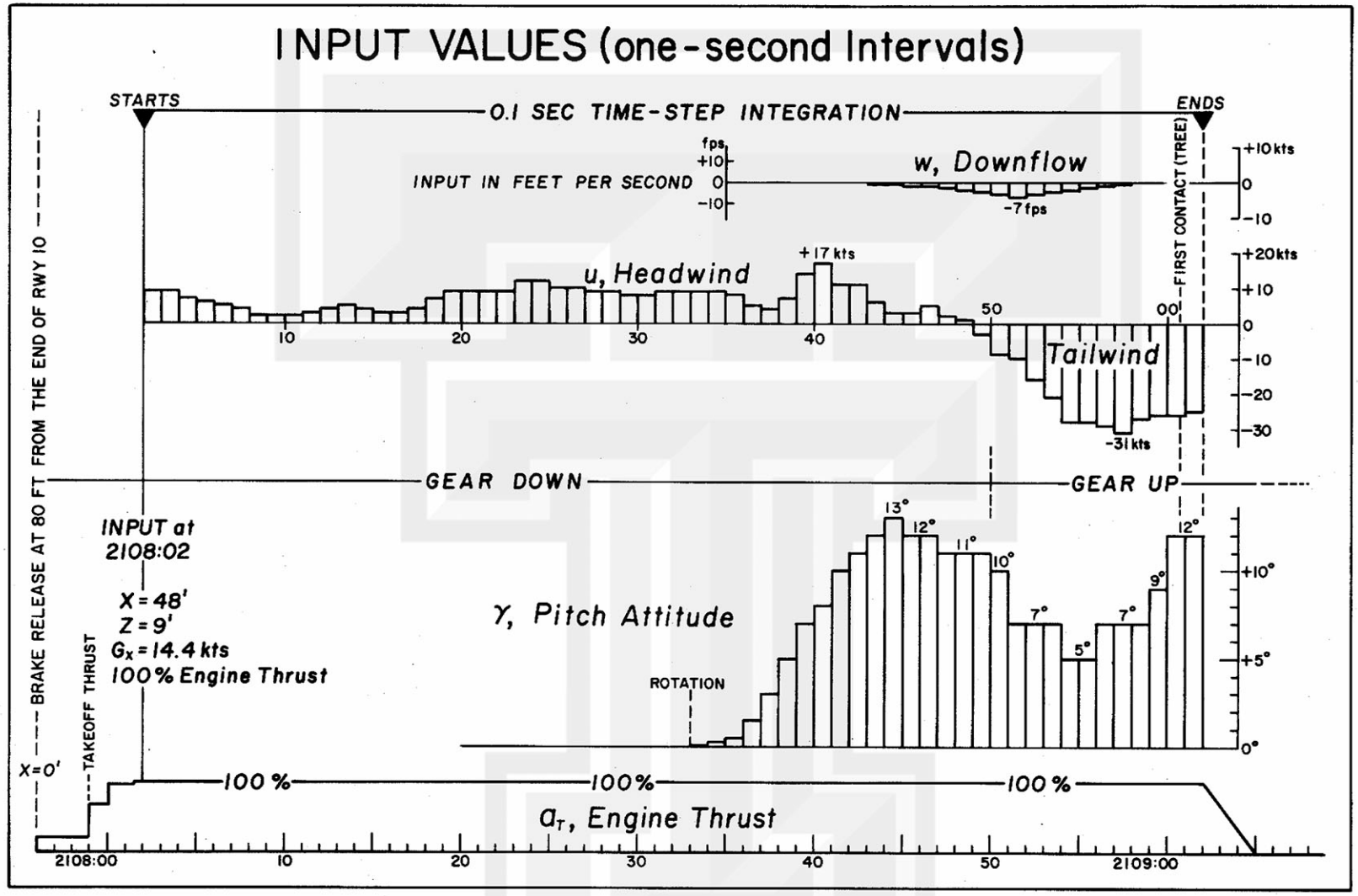

Fig.12 Input values given as a function of time at one-minute intervals. Pitch attitude, horizontal wind, and vertical wind were chosen to be the input parameters. They were changed in each iterated computation until the output data finally satisfied the 8 constraints listed in Section 3.

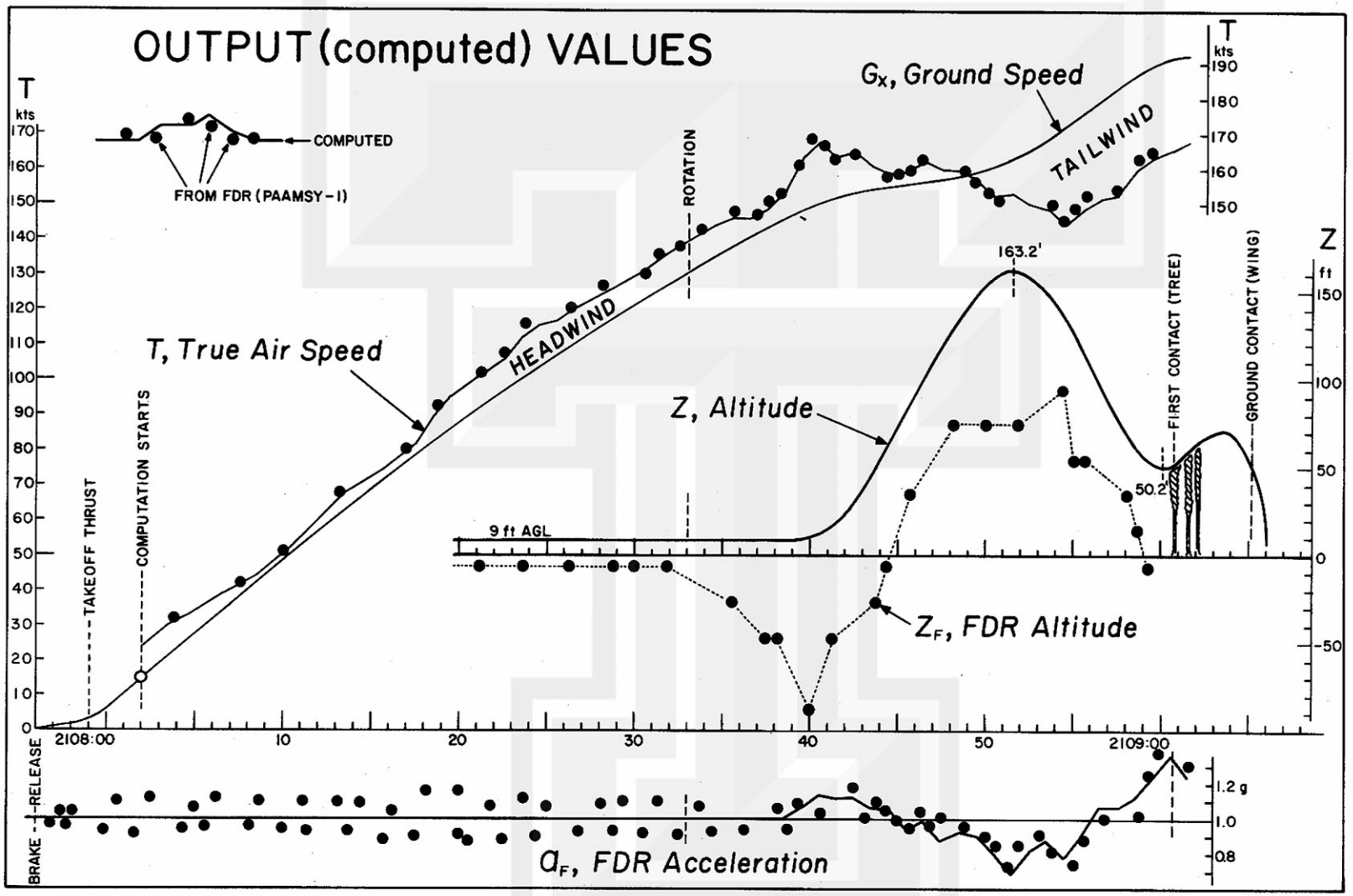

Fig.13 Output values obtained after the 27 iterative computations. Computed values are indicated with lines and FDR values, with black circles. It should be noted that tailwind which reduces aircraft's true air speed increases significantly the kinetic energy of the aircraft.

5 Microburst Penetration by PAA 759

The headwinds presented in Table 3 at one-second intervals were combined with the crosswinds computed from

$$v = G'_X \tan \delta \tag{34}$$

where v is crosswind perpendicular to the ground speed G'_X and δ the drift angle.

By combining u and v, the total horizontal wind speeds W at the flight altitude, Z were computed from

$$W = (u^2 + v^2)^{\frac{1}{2}} \tag{35}$$

They were then reduced to the 30 ft winds by using the wind-height equation applicable to the microburst. The equation is

$$W_Z = \sin \frac{\pi}{2} (Z/100)^{0.3} \tag{36}$$

where Z denotes the height above the runway. This equation can be used to determine

$$W_{30'} = W_Z \frac{\sin \frac{\pi}{2}(30/100)^{0.3}}{\sin \frac{\pi}{2}(Z/100)^{0.3}} \tag{37}$$

The cross-runway angles, θ of the winds were computed from

$$\theta = \tan^{-1} \left[\frac{v}{u}\right]_{at\ 30'} \tag{38}$$

in order to plot the wind vectors printed in red in Fig. 14.

Dashed lines with arrowhead denote outflow winds which were expanding radially from the microburst center located inside the runway triangle to the north of the terminal building. Isotachs, lines of equal wind speed, reveal that strong microburst winds were pushing toward the northeast, inducing 15 to 20 kt winds from the south experienced by Capt. Fagan, piloting a Cessna Citation. Mrs. Anglin, while driving south on Williams Boulevard, experienced strong westerly winds when PAA crossed the boulevard.

The centerfield anemometer reported the 15 kts wind which came from the direction of the microburst center. LLWSAS East anemometer located near the first contact tree reported the 6 kts wind from 310°. This wind speed is too low in relation to the 25 kts estimated in this paper, as well as the strong westerly wind witnessed by Mrs. Anglin.

Divergence of the horizontal wind at 30 ft was computed, based on the radial outflow assumption which is reasonable in this case. Values were computed at one-second intervals from

$$\text{div } W_{30'} = \frac{W_{30'}}{R} + \frac{dW_{30'}}{dR} \tag{39}$$

where $W_{30'}$ denotes the wind at 30 ft above the runway 10 and R, the distance from the microburst center to the aircraft track.

Fig. 15 reveals the vertical cross section of the horizontal wind penetrated by the aircraft along the black line with two peak altitudes. It will be seen that the aircraft lifted off rapidly upon reaching the region of a strong headwind. Upon entering the tailwind near the peak altitude, the plane began sinking rapidly to its lowest altitude just before the first contact.

The vertical motion field presented in Fig. 16 was computed by integrating the divergence equation upward, while changing the wind speed as a function of the height in Eq. (36). This figure reveals that the maximum altitude of the aircraft was located at the downflow center with its descending speed of 7.4 ft per second.

The vertical cross section of microburst winds in Fig. 17 shows the feature of a downflow which split into two, the one moving toward the front side and the other toward the rear side. The split is caused by the stagnation cone of the air which piles up on the ground as the velocity head of the downflow is being converted into the pressure head.

The front surface of the stagnation cone acts as a boundary surface on which the vertical current slides down while changing its flow direction from near vertical to horizontal. During the mature stage of a microburst, the maximum horizontal speed is located 50 to 150 ft above the ground. Curling motions of dust cloud were observed during the JAWS project, suggesting that a vortex ring with its horizontal axis encircles the stagnation cone. Such a vortex ring will bring the height of the maximum outflow wind very close to the ground.

The rear side of the microburst is less impressive. However, a small branch of the rear outflow induced a 17 kts headwind at 2108:40, giving rise to the positive climb callout at 2108:41.

The horizontal scale of the microburst at the accident time was slightly less than 2 n.m.. A misoscale disturbance, such as this microburst, cannot always be detected in time for an effective warning based solely on ground-based anemometers.

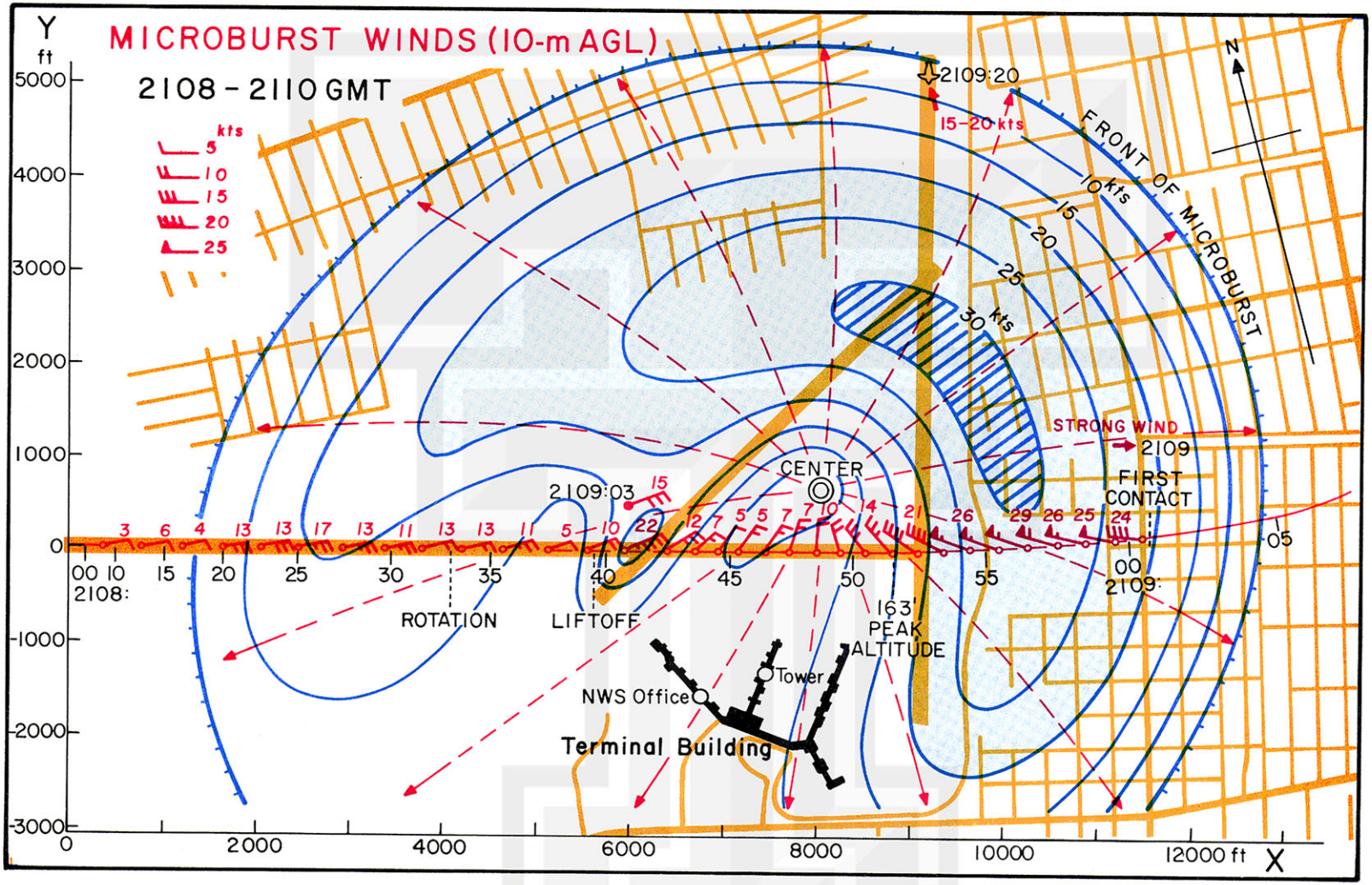

Fig.14 Windfield of the microburst over the New Orleans International Airport (Moisant Airport) at the time of the accident. All wind speeds with barbs are reduced to the 30 ft (10 m) height above the runway with 0 to +1 ft elevation. Microburst was moving towards the northeast accompanied by strong west winds near the accident site and 15 to 20 kts southerly wind at the departure end of runway 19.

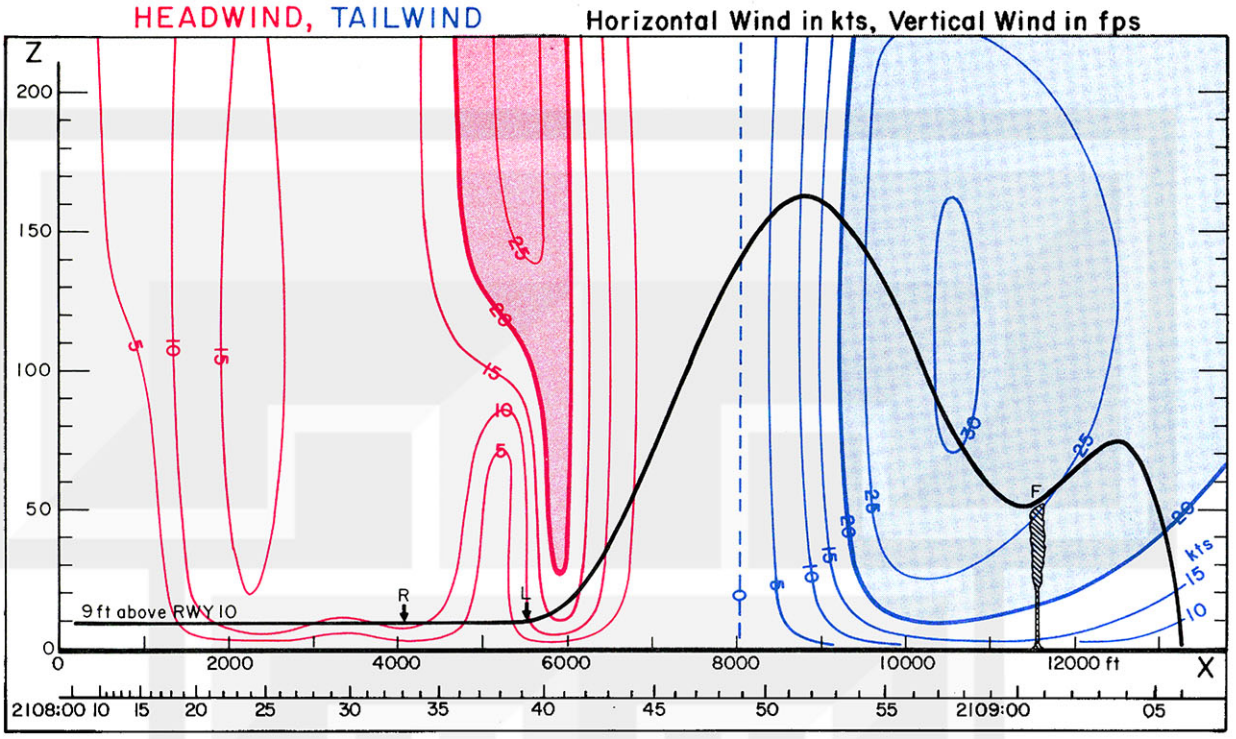

Fig. 15 Vertical cross section of both headwind (red) and tailwind (blue) at the time of the accident. Letter R denotes rotation, L the liftoff point, and F the first contact tree.

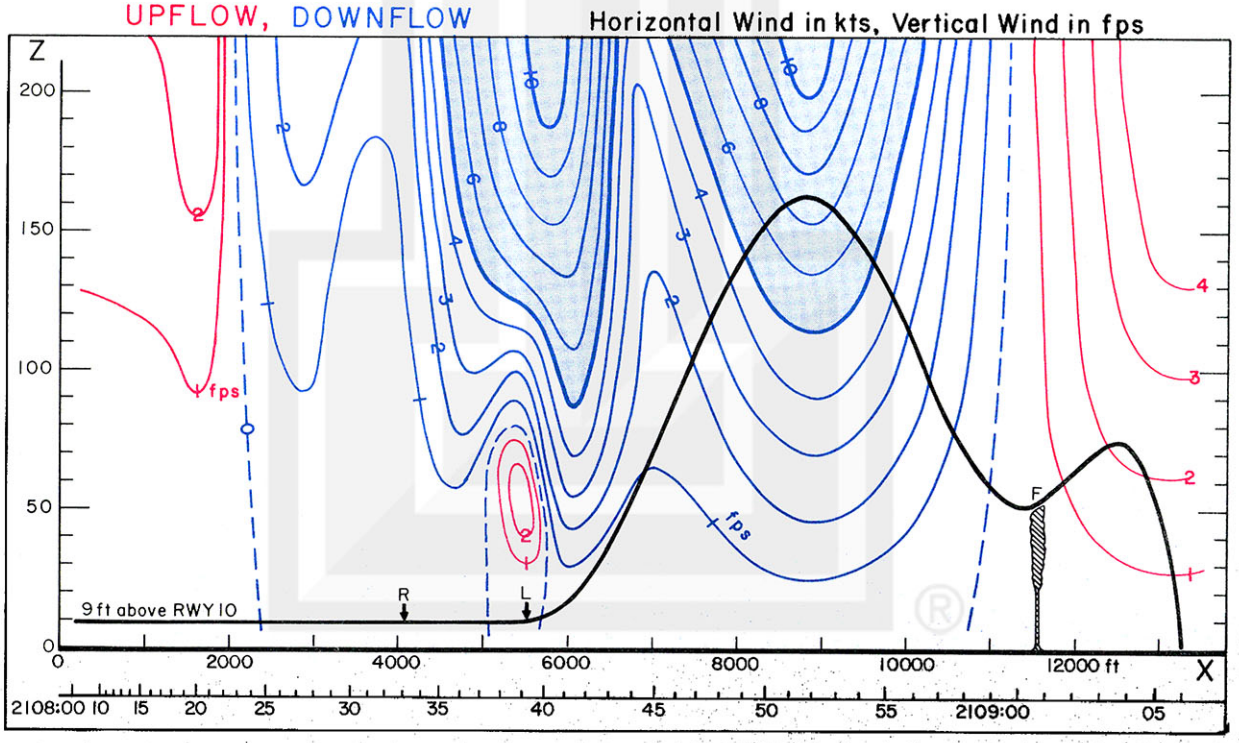

Fig.16 Vertical cross section of the vertical wind computed from the equation of continuity under the radial flow assumption from the microburst center. Both dW/dR and W/R effects were taken into consideration.

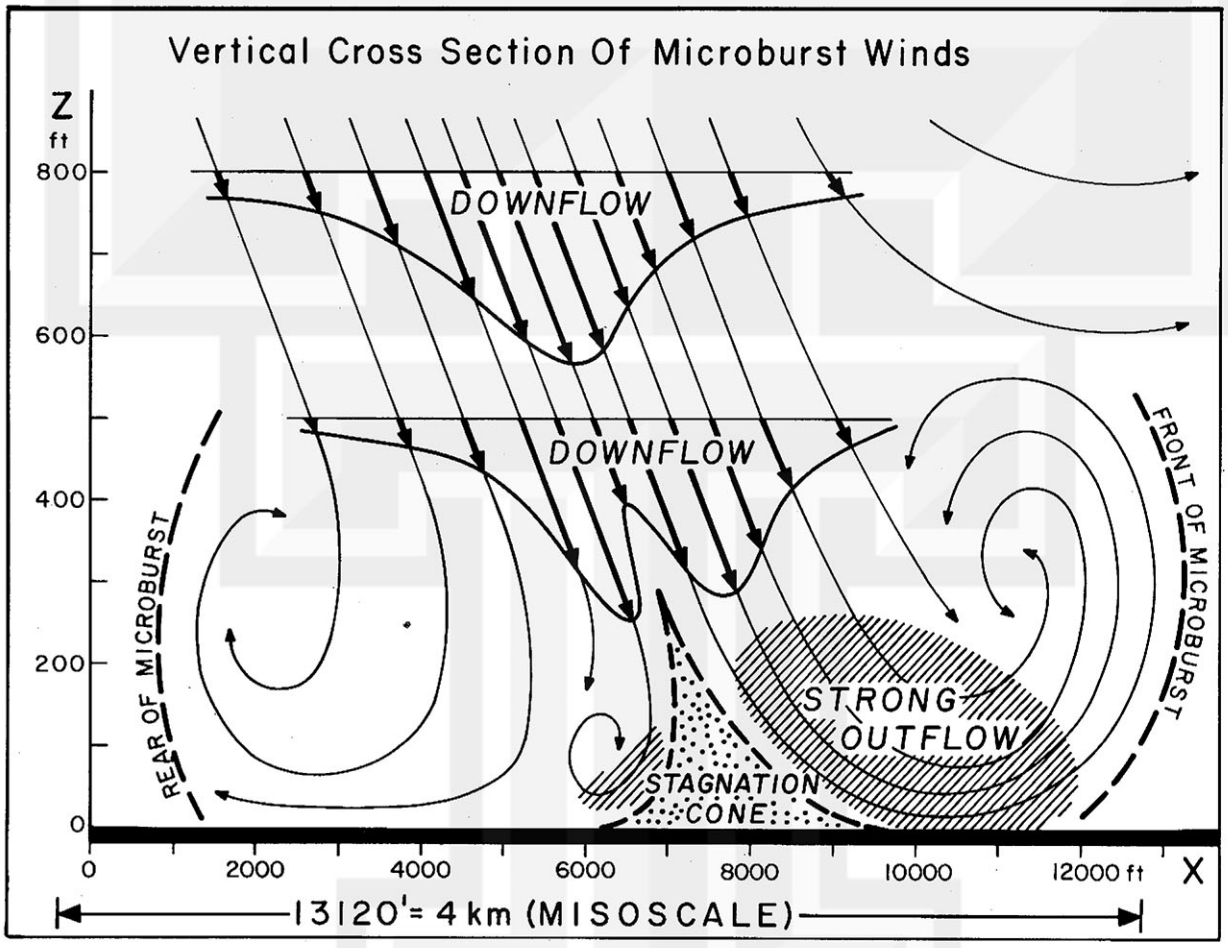

Fig.17 Vertical cross section of the microburst wind on the coordinates with 1 to 10 vertical exaggeration. Two downflows in Fig. 16 are resulted by the split flow on both sides of the stagnation cone located near the impact point of the microburst. NIMROD and JAWS data analyses show that the outflow speed is several times faster than the downflow speed at 300 ft above the ground.

6 Effects of Horizontal and Vertical Wind Shear

It has been confirmed that the aircraft under investigation lost its altitude at the location of the strong downflow within the microburst. As implied by Eq. (39), it is likely that the downflow is located where the head- to tailwind shear is the strongest.

Effect of the Tailwind and Downflow

In order to estimate the effect of downflow and tailwind, both together or separately, a set of computer simulations was performed. Their combinations, identified as cases A, B, C, and D, include different wind shears while pitch attitudes were kept unchanged. Case A includes both tailwind and downflow, while case D is free from wind shear.

Cases	Tailwind	Downflow
A	yes	yes
B	yes	no
C	no	yes
D	no	no

The result of the simulations in Fig. 18 is of extreme interest. By eliminating downflow from wind shear (case B), the aircraft with identical pitch attitude did fly out of the microburst. The loss of altitude due to the downflow was 50 ft. The difference between cases C and D also resulted in a 50 ft loss of altitude, suggesting that a 50 ft loss is expected to occur irrespective of the horizontal wind shear.

The effect of the horizontal wind shear between B and D is 101 ft. It should be noted that the effect of the horizontal wind shear between C and A is also 101 ft, suggesting that a 101 ft loss of altitude occurs irrespective of the downflow wind shear.

Effect of the Microburst Strength

The second set of computer simulations was produced by changing the microburst strength while keeping the pitch attitude (as a function of time) constant. The strength was changed by multiplying various factors (in %) to both horizontal and vertical wind speeds. These factors are selected to be 200% (very strong), 150%, 125% (stronger), and 100% (original), 75% (weaker) and 50% (very weak) in order to generate all intensities of microbursts.

The results summarized in Fig. 19 reveal that PAA 759 could have flown out of the microburst if it was 25% weaker than the original strength. If the microburst was 25% stronger or 125% of the original strength, the minimum altitude would have been only 15 ft above the ground. At 150% and 200% strength, micro-

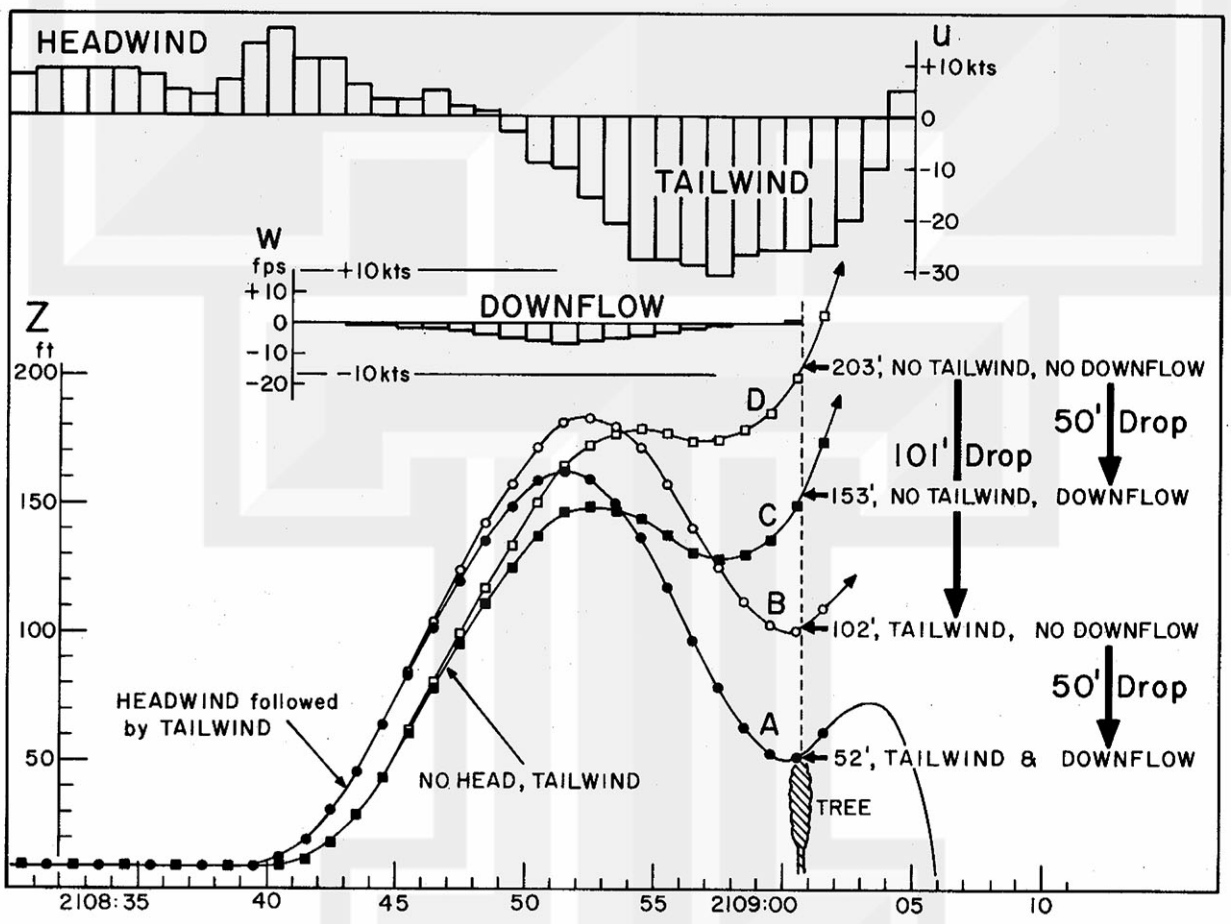

Fig.18 Effect of tailwind and downflow upon aircraft trajectories. At the location of the first impact tree, aircraft lost 101 ft altitude due to the tailwind, while the downflow of only up to 7 fps caused the 50-ft drop. This computation shows that the aircraft could have flown over the tree if either the downflow or the tailwind did not exist.

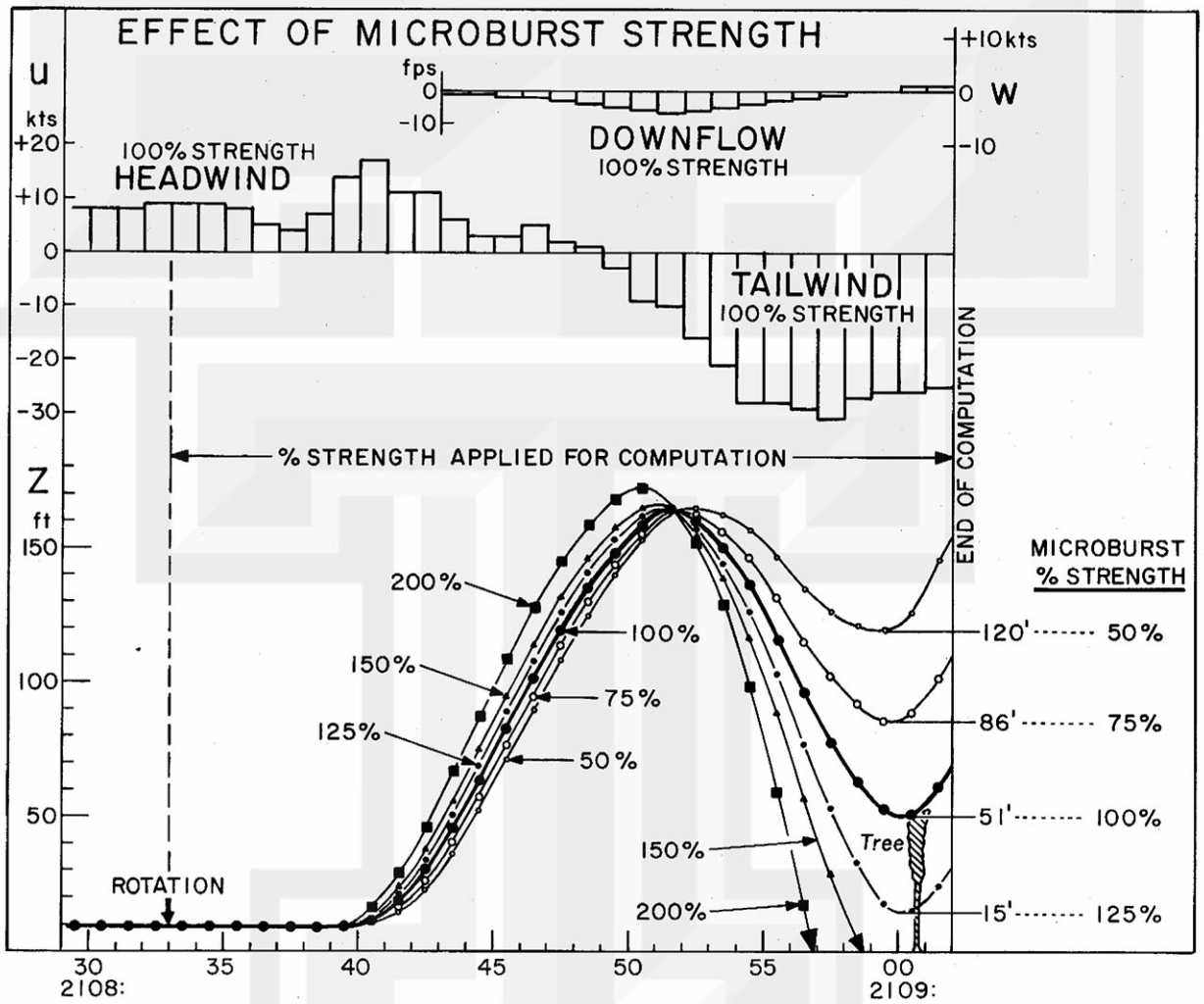

Fig.19 Effect of the strength of microburst upon aircraft trajectories. In this simulation, the actual wind speeds of the microburst were prorated by the factors of 50%, 75%, 125%, 150%, and 200%. The 200% strength microburst is characterized by the 14 fps downflow and 62 kts tailwind. In this extreme case, the aircraft descended straight to the ground. On the other hand, the 75% strength microburst permitted the aircraft to fly over the tree at 86 ft elevation.

bursts could bring the aircraft down to the ground within a short time.

Gust Frontal Wind Shear, a Life Saver

Gust fronts have been considered to be an inducer of a dangerous wind shear. In spite of this common belief, Republic 632 which departed from runway 19 at 2101 GMT gained its air speed and altitude during the penetration through a gust front. Refer to the author's 1981 article "Microburst as an aviation wind shear hazard" (reference on the back page).

As shown in Fig. 6, REP 632 took off in a 10 to 13 kt wind from the east-northeast which acted as a strong crosswind and a weak tailwind. IAS fluctuated 100 kts-110 kts-100 kts-105 kts-100 kts. It rotated at 121 kts IAS (V1 = 132 kts, V2 = 140 kts). Apparently, the aircraft flew into a gust front over the end of RWY 19, resulting in an increase in IAS to 160 kts almost instantly. The co-pilot said that he had never seen air speed boil up so fast.

In an attempt to simulate the effect of a hypothetic gust front on PAA 759, a set of computer simulations was performed. In these simulations, a gust front was placed in front of the aircraft at three different locations: -- at the moment of rotation, 8 seconds after the rotation, 16 seconds after the rotation when the aircraft reached 142 ft altitude, and several seconds before the first impact.

Fig. 20 reveals that the gust front greatly enhanced the climb capabilities in all cases. The frontal passage at the time of the rotation turned out to be most effective. The liftoff time was almost as effective. The encounter at 142 ft was early enough to increase the aircraft altitude to 317 ft above the first impact tree. Even a gust front introduced only 3 to 4 seconds prior to the first contact initiated an immediate altitude gain of the aircraft.

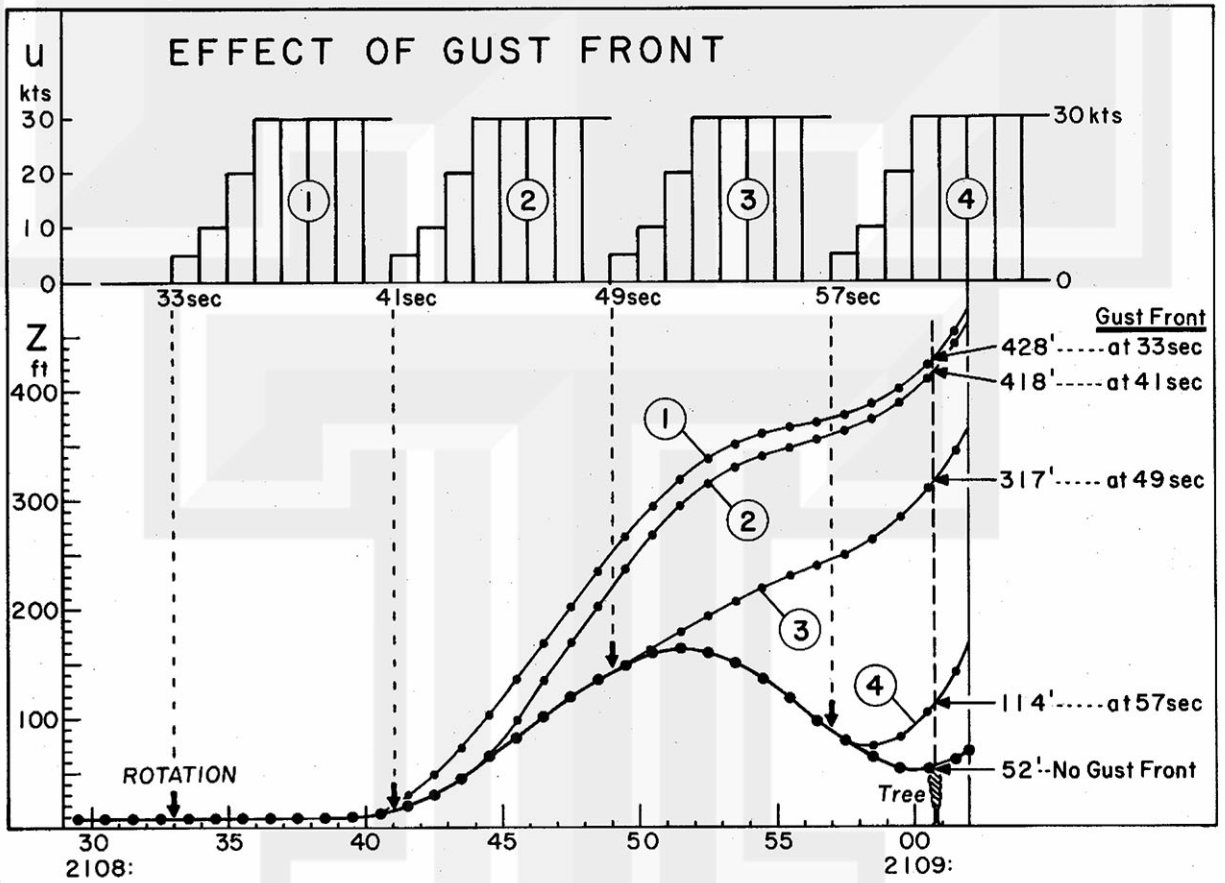

Fig.20 Effect of gust-front winds upon aircraft trajectories. In this simulation, the time of the onset of a gust front was moved from rotation to near liftoff, etc. In all cases, the gust front acted as the life saver. As an inducer of turbulence, one should beware of the gust front. In terms of wind shear, a gust front is extremely favorable in gaining aircraft altitude. Refer to Fujita (1981) Microburst as an aviation wind-shear hazard.

7 Conclusions

The purpose of this research is to determine the nature of the wind shear existed over the New Orleans International Airport when PAA 759 lost its altitude, leading to the first impact on trees. As in most other accident cases, investigators, such as this author, always suffer from the shortage of reliable data. Nonetheless, an attempt was made to reconstruct the short flight by introducing eight constraints including the equation of continuity. Finally, a unique solution satisfying all constraints was obtained after going through 27 iterative computations.

Computer simulations revealed that the accident aircraft flew into a +17 kts head- to -31 kts tailwind accompanied by a -7 fps downflow. The disturbance of the wind shear was identified to be a microburst approximately 2 n.m. across.

The loss of altitude inside the microburst was attributed 2/3 to the tailwind and 1/3 to the downflow. If one of these causes had not been present, the aircraft could have flown out of the microburst.

The strength of the microburst also played an important role in the aircraft trajectory. Simulations performed by changing the microburst strength indicated that the aircraft could have escaped the microburst if it had been 25% weaker than it was.

Finally, the effect of the gust front, such as was penetrated by Republic 632 at 2101 GMT, was determined through computer simulations. Irrespective of the time of the encounter, the accident aircraft did fly out of the microburst when an artificial gust front was added at various phases of the takeoff operation.

ACKNOWLEDGEMENTS:

▲Basic equations for the aircraft performance were developed under the National Science Foundation Grant, NSF ATM 81-09828 as a part of the JAWS research being conducted at the University of Chicago. ▲Satellite photo analysis reported in this paper is a portion of the ongoing research of rapid scan data supported by the National Environmental Satellite Service under Grant, NOAA NA 80 AA-D-00001. ▲Research on the accident leading to the publication of this paper was supported by Pan American World Airways, Inc.

Sincere appreciation is due to Mr. Arnold Reiner, Manager - Flight Safety Analysis and Information and Mr. Ernie N. Tangren, Operations Engineer, Pan American World Airways, Inc. for their assistance and advise in reconstructing the PAA 759 flight path.

The Author is also grateful to Mr. William H. Haggard, Climatological Consultant Corporation for his continuous assistance in obtaining and analyzing the vital meteorological data. During Christmas and New Year Holidays, staff members of SMRP assisted the author in all possible means toward the completion of this paper before the beginning of the Winter, 1983 Quarter.

Question and Answer

Numerous questions have been asked since the author introduced the term "DOWNBURST" in March 1976. Questions presented in this section were selected from those asked by pilots, meteorologists and my students. If the readers wish to ask specific questions, please send them directly to the author.

Q: In your JFK accident paper, you called the storm a "downburst", but now you identify the New Orleans storm "microburst". What is the difference?

A: When I first identified as a "downburst" in 1976, based on the JFK accident, I did not know the size distribution. Numerous downbursts were investigated since then, including a 166-mile long and 17-mile wide giant downburst in Wisconsin, a 1.5 mile diameter downburst inside Denver's Stapleton Airport, etc. Now I call large (mesoscale) downbursts "macrobursts" and small (misoscale) downbursts "microburst". Both macroburst and microburst belong to the downburst family.

Q: Why is the microburst important for aviation?

A: A microburst is very small and short lived, lasting no more than 5 minutes. It cannot be predicted and is hard to detect until it becomes too late to fly out.

Q: How about macrobursts?

A: The National Weather Service worries about the macrobursts, because they could produce serious damage like that of tornadoes. Most airports are closed for 5 to 20 minutes during the passage of a strong macroburst.

Q: What does a microburst look like from the cockpit?

A: It looks like a localized shower, either heavy or very light. There is no way of knowing if the root of the shower is inducing (or will induce) microburst winds.

Q: What is the first indication that I am flying straight into a microburst?

A: An indication is the unusual increase in the air speed / aircraft altitude while approaching a shower, which may look either bad or innocent. Both downflow and tailwind shear could be waiting only a few seconds away.

Q: How does the angle of attack change in a microburst penetration?

A: When the headwind increases during the approach, both angle of attack and air speed increase together. The aircraft gains altitude. At the dead center of the microburst, there is no headwind or tailwind, but the downflow will decrease the angle of attack. During the fly-out phase, you encounter both downflow and tailwind simultaneously. Air speed and angle of attack decrease together, resulting in a serious loss of altitude.

Q: Can you describe these changes more quantitatively?

A: Right now I cannot, because net changes are dependent upon your pitch attitude and the strength of the wind shear, as well as the ground speed of the aircraft. Within several months, however, I will be completing computer simulations which will give us exact quantitative values.

Q: It is best not to fly into a microburst. How early can you detect a microburst which endangers aircraft operations at low altitude?

A: In my view, most of the Denver-type dry microbursts can be detected by a single Doppler radar 2 to 3 minutes before the onset of microburst winds. A microburst in a wet area, such as the New Orleans storm, is very hard to detect, because the mechanism of the microburst formation has not been known.

Q: What is the difference between downdraft and downburst?

A: Downdraft is the mid-air downflow and downburst is the near-ground winds. Most downdrafts, weak or strong, lose downflow speed long before reaching the near-ground height. Only one downdraft out of several hundreds descends close to the ground to induce strong head- and tailwind shear.

Q: Can you identify which downdrafts will reach near the ground to induce microbursts?

A: Unfortunately, nobody can.

Q: Do microbursts always produce rain on the ground?

A: The answer to this question is no. 85% of the JAWS microbursts produced no rain on the ground (dry microburst) and 48% of the NIMROD microbursts were dry.

Q: How much rain do you expect in a very wet microburst?

A: The wettest microburst in JAWS produced 0.24 inch in 4 minutes or 3.6 inches per hour rate. In NIMROD, the wettest one was 0.58 inch in 4 minutes or 8.7 inches per hour. In a very wet microburst, an aircraft may disappear in heavy rain during its climbout phase.

Q: Is dry microburst generally weaker than wet microburst?

A: No, it is not always the case. The strongest JAWS microburst with 57 mph wind was a dry microburst. An innocent-looking shower or virga in the Denver area could induce 40 to 60 mph winds.

Q: How often do we experience microbursts at a given location?

A: Although we have no national statistics, 4 microbursts per month occurred at Denver's Stapleton Airport and 2 microbursts per month at Chicago's O'Hare Airport according to the JAWS and NIMROD statistics.

Q: Why do you expect to find raindrops in a dry microburst?

A: In the dry microburst, raindrops evaporate before reaching the ground. It is seen as a virga consisting of wisps or streaks of falling droplets.

"About the author"

TETSUYA THEODORE FUJITA

Born on October 23, 1920 at Kitakyushu City, Japan

1953 • D. Sc. from Tokyo University, Tokyo, Japan
1953 • Research Associate, Department of Meteorology, University of Chicago
1956 • Director, Mesometeorology Research Project, University of Chicago
1962 • Associate Professor, Dept. of Geophysical Sciences, Univ. of Chicago
1965 • Professor, Department of Geophysical Sciences, University of Chicago
1968 • Became a U.S. Citizen

Membership:

- American Meteorological Society, Fellow since 1968
- American Geophysical Union, Fellow since 1973
- Meteorological Society of Japan
- National Weather Association

Wind-shear related Awards:

1977 • Admiral Luis de Flores Flight Safety Award, Flight Safety Foundation
1977 • Distinguished Service Award, Flight Safety Foundation
1979 • Distinguished Public Service Medal, NASA
1982 • Losey Atmospheric Sciences Award, AIAA

Wind-shear related Publications:

1976 • Spearhead echo and downburst near the approach end of a John F. Kennedy Airport runway, New York City. SMRP Res. Paper 137, Univ. of Chicago, 51pp.

1977 • Spearhead echo and downbursts in the crash of airliner. Monthly Weather Review, 105, 129-146. (Fujita and Byers)

1977 • Analysis of three weather-related aircraft accidents. Bulletin of American Meteorological Society, 58, 1164-1181. (Fujita and Caracena)

1977 • Common denominator of three weather-related aircraft accidents. Preprint, 10th Conf. on Severe Local Storms, Omaha, 135-142. (Fujita and Caracena)

1978 • Wind shear at Dulles Airport on 18 May 1977. SMRP Res. Paper 159, University of Chicago, 19pp.

1980 • Downbursts and microbursts - An aviation hazard. Preprints, 19th Conf. on Radar Meteorology, Miami Beach, Fla., 94-101.

1981 • Microburst as an aviation wind-shear hazard. Preprint, 19th Aerospace Science Meeting, St. Louis, AIAA-81-0386, 9pp.

1981 • Five scales of airflow associated with a series of downbursts on 16 July 1980. Monthly Weather Review, 109, 1438-1456. (Fujita and Wakimoto)

1981 • Tornadoes and downbursts in the context of generalized planetary scale. Journal of Atmospheric Sciences, 38, 1512-1534.